

AD-A042 374

GENERAL ELECTRIC CO SYRACUSE N Y HEAVY MILITARY EQUI--ETC F/G 4/1  
AN ANALYSIS OF IONOSPHERIC ELECTRON CONTENT MEASUREMENTS UTILIZ--ETC(U)  
DEC 74 G H MILLMAN

UNCLASSIFIED

R74EMH24

NL

1 of 1  
ADA042374



END  
DATE  
FILMED  
8-77  
DDC

AD A 042374

5

6

AN ANALYSIS OF IONOSPHERIC ELECTRON CONTENT  
MEASUREMENTS UTILIZING SATELLITE-EMITTED SIGNALS

14

R74EMH24

10

George H. Millman

11

December 1974

12

84p.

DDC  
AUG 2 1977

General Electric Company  
Syracuse, New York 13201

AD No. \_\_\_\_\_  
DDC FILE COPY

DISTRIBUTION STATEMENT A  
Approved for public release;  
Distribution Unlimited

408 969

4B

## GENERAL ELECTRIC COMPANY TECHNICAL INFORMATION

Within the limitations imposed by Government data export regulations and security classifications, the availability of General Electric Company technical information is regulated by the following classifications in order to safeguard proprietary information:

### CLASS 1: GENERAL INFORMATION

Available to anyone on request.  
Patent, legal and commercial review  
required before issue.

### CLASS 2: GENERAL COMPANY INFORMATION

Available to any General Electric Company  
employee on request.  
Available to any General Electric Subsidiary  
or Licensee subject to existing agreements.  
Disclosure outside General Electric Company  
requires approval of originating component.

### CLASS 3: LIMITED AVAILABILITY INFORMATION

Original Distribution to those individuals with  
specific need for information.  
Subsequent Company availability requires  
originating component approval.  
Disclosure outside General Electric Company  
requires approval of originating component.

### CLASS 4: HIGHLY RESTRICTED DISTRIBUTION

Original distribution to those individuals personally responsible for the Company's interests in the subject.  
Copies serially numbered, assigned and recorded by name.  
Material content, and knowledge of existence, restricted to copy holder.

GOVERNMENT SECURITY CLASSIFICATIONS, when required, take precedence in the handling of the material. Wherever not specifically disallowed, the General Electric classifications should also be included in order to obtain proper handling routines.

TIS Distribution Center  
 CSP 4-24, X7712  
 Syracuse, New York 13201



HEAVY MILITARY EQUIPMENT DEPARTMENT

TECHNICAL INFORMATION SERIES

Author G. H. Millman	Subject Category Beacon Satellite, Ionospheric Electron Content	No. R74EMH24 ✓
		Date Dec 1974
Title AN ANALYSIS OF IONOSPHERIC ELECTRON CONTENT MEASUREMENTS UTILIZING SATELLITE-EMITTED SIGNALS		
Copies Available at HMED TIS Distribution Center Box 1122 (CSP 4-24) Syracuse, New York 13201	GE Class 1	No. of Pages 82
	Govt Class Unclassified	
Summary Analytical techniques are available which make use of the Faraday polarization rotation and the Doppler frequency shift phenomena for determining the ionospheric electron content by the passive monitoring of radio wave transmissions emanating from earth satellites. The accuracy of the various techniques can be evaluated by the simulator-computer program described in this report. The major components of the simulator consist of a satellite-orbit generator, a time-variant three-dimensional electron density model and an earth magnetic field model expressed in terms of a series of spherical harmonics. Ray tracings are performed utilizing Simpson's rule for numerical integration of the definite integrals defining the propagation phenomena. Preliminary results are presented of an analysis performed for one location in the midlatitudes.		
Key Words Ionosphere                      Doppler Frequency Shift Electron Content              Differential Phase Faraday Rotation              Satellite		

This document contains proprietary information of the General Electric Company and is restricted to distribution and use within the General Electric Company unless designated above as GE Class 1 or unless otherwise expressly authorized in writing.

Send to \_\_\_\_\_  
 \_\_\_\_\_  
 \_\_\_\_\_

GENERAL ELECTRIC COMPANY  
HEAVY MILITARY EQUIPMENT DEPARTMENT  
TECHNICAL INFORMATION SERIES

SECTION Information Systems Engineering  
 UNIT 450  
 HMES ACCOUNTING REFERENCE \_\_\_\_\_  
 COLLABORATORS \_\_\_\_\_  
 APPROVED J. P. Chiasson TITLE Mgr., ISE LOCATION CSP 9-25  
J. P. Chiasson

TIS R74EMH24

MINIMUM DISTRIBUTION - Government Unclassified Material (and Title Pages) in G.E. Classes 1, 2, or 3 will be the following.

Copies	Title Page Only	To
0	1	Legal Section, HMED (Syracuse)
0	1	Manager, Technological Planning, HMED (Syracuse)
5	6	G-E Technical Data Center (Schenectady)
5	(First Class Only)	Defense Documentation Center, Cameron Station, Alexandria, Va. 22314

MINIMUM DISTRIBUTION - Government Classified Material, Secret or Confidential in G.E. Classes 1, 2, or 3 will be the following.

1	1	Classified Section, Electronics Park Library
1	0	Manager, Technological Planning, HMED (Syracuse)

ADDITIONAL DISTRIBUTION (Keep at minimum within intent of assigned G.E. Class.)

COPIES	NAME	LOCATION
--------	------	----------

## TABLE OF CONTENTS

<u>Section</u>	<u>Title</u>	<u>Page</u>
I	INTRODUCTION	1-1
II	THEORETICAL CONSIDERATIONS	2-1
	2.1 Faraday Rotation	2-1
	2.1.1 Introduction	2-1
	2.1.2 Single Frequency Method	2-2
	2.1.3 Two Frequency Method	2-3
	2.1.4 Differential Polarization Rotation Angle Method	2-3
	2.1.5 Polarization Rotation Rate Method	2-4
	2.1.6 Least Square Method	2-5
	2.2 Differential Phase and Doppler Frequency Shift	2-6
	2.2.1 Introduction	2-6
	2.2.2 Doppler Frequency Shift Method	2-7
	2.2.3 Doppler Frequency Slope Method	2-8
	2.2.4 Ionosonde Method	2-8
	2.3 Faraday Rotation - Differential Doppler	2-11
III	COMPUTER SIMULATION OF SATELLITE TRANSMISSIONS	3-1
IV	SIMULATOR - DATA ANALYSIS	4-1
V	CONCLUSIONS	5-1
VI	REFERENCES	6-1
	APPENDIX A Faraday Polarization Rotation Effect	A-1
	APPENDIX B Differential Phase and Doppler Frequency Shift	B-1
	APPENDIX C Ionospheric Index of Refraction	C-1

ACQUISITION	
THIS	Write Section <input checked="" type="checkbox"/>
OR	Both Section <input type="checkbox"/>
UNASSIGNED	<input type="checkbox"/>
INVESTIGATION	<i>for file</i>
BY	<i>file</i>
DISTRIBUTION, AVAILABILITY CENTER	
NO.	AVAIL. NO. OF SPECIAL
<b>A</b>	

## LIST OF ILLUSTRATIONS

<u>Figure</u>	<u>Title</u>	<u>Page</u>
3-1	Logic Block Diagram of Faraday-Doppler Simulator	3-2
4-1	Earth Trace of the Orbit of TRANSIT Satellite, Object No. 1970-067A, June 3, 1974 and Geographic Coordinate - Location of Vertical Distributions of Electron Density	4-2
4-2	Altitude and Angular Coordinates of TRANSIT Satellite, Object No. 1970-067A, June 3, 1974, as Predicted for Schenectady, New York	4-3
4-3	Vertical Distribution of Electron Density Along the 74.07°W Meridian at 1800 Hours GMT, June 3, 1974 as Predicted by the Penn State Ionosphere Model	4-4
4-4	Electron Content on June 3, 1974, as Predicted by the Penn State Ionosphere Model	4-6
4-5	Simulated Faraday Polarization Rotation Angle of TRANSIT Satellite, Object No. 1970-067A, June 3, 1974	4-7
4-6	The Parameters M and $H \cos \theta$ in the Direction of Ambiguous Faraday Rotation of $\pi/2$ Radians at 400 MHz	4-8
4-7	Error in Determining the Vertical and Slant Electron Content in the Direction of Ambiguous Faraday Rotation of $\pi/2$ Radians at 400 MHz By the Single Frequency Method	4-9
4-8	The Parameters M and $H \cos \theta$ in the Direction of Ambiguous Faraday Rotation of $\pi/4$ Radians at 400 MHz	4-11
4-9	Error in Determining the Vertical and Slant Electron Content in the Direction of Ambiguous Faraday Rotation of $\pi/4$ Radians at 400 MHz By the Single Frequency Method	4-12
4-10	The Parameters M and $H \cos \theta$ in the Directions of Faraday Rotation Difference of $\pi/2$ Radians at 150 MHz	4-14
4-11	Error in Determining the Vertical and Slant Electron Content at 150 MHz by the Differential Polarization Rotation Angle Method	4-15
4-12	Geometric Magnetic Factor, M, As a Function of Altitude Across the Satellite Orbital Pass	4-17
4-13	Magnetic Function, $H \cos \theta$ , As a Function of Altitude Across the Satellite Orbital Pass	4-18
4-14	Time Derivative of the Parameters M and $H \cos \theta$	4-19
4-15	Error in Determining the Vertical and Slant Electron Content at 150 MHz by the Polarization Rotation Rate Method	4-21

LIST OF ILLUSTRATIONS (Cont)

<u>Figure</u>	<u>Title</u>	<u>Page</u>
4-16	Simulated Relative Phase Difference Between 150- and 400-MHz Transmissions from TRANSIT Satellite, Object No. 1970-067A, June 3, 1974	4-22
4-17	Simulated Free Space - Doppler Frequency Shift of 150- and 400-MHz Transmissions from TRANSIT Satellite, Object No. 1970-067A, June 3, 1974	4-23
4-18	Simulated Ionospheric Doppler Frequency Shift of 150- and 400-MHz Transmissions from TRANSIT Satellite, Object No. 1970-067A, June 3, 1974	4-24
4-19	Electron Density Profile at Point of Closest Approach of TRANSIT Satellite, Object No. 1970-067A, 1800 Hours GMT, June 3, 1974 at Schenectady, New York as Predicted by the Penn State Ionosphere Model and Ionosonde Method	4-29
4-20	Time Derivative of the Parameters M and $H \cos \theta$ in the Direction of Differential Phase Reversal	4-31
4-21	Error in Determining the Vertical and Slant Electron Content at 150 MHz by the Faraday-Doppler Hybrid Method	4-32

## LIST OF TABLES

<u>Table</u>	<u>Title</u>	<u>Page</u>
4-1	Parameters Used in the Evaluation of the Accuracy of the Polarization Rotation Rate Method	4-20
4-2	Error Estimation of the Doppler Frequency Shift Method	4-26
4-3	Error Estimation of the Doppler Frequency Slope Method	4-27
4-4	Error Estimation of the Ionosonde Method	4-28
5-1	Altitude of $\bar{M}$ and $\overline{H \cos \theta}$ Evaluation for Zero Percent Error in Ionospheric Electron Content Estimation	5-2
5-2	Error in Ionospheric Electron Content Estimation Due to Mean Field Height Inaccuracy	5-3
5-3	Error in Ionospheric Electron Content Estimation Utilizing Dispersive Phase-Doppler Technique	5-4

## SECTION I

### INTRODUCTION

When radio waves emanating from earth's satellites traverse the ionosphere, they undergo both a rotation of the plane of polarization, i.e., Faraday effect, and a Doppler frequency shift. Analytical techniques have evolved which utilize the two phenomena for the study of the electron content in the ionosphere.

Utilization of the Faraday method which necessitates that the satellite-transmitted signal be linearly polarized has been demonstrated by Bertin and Papet-Lépine (1970), Bertin et al. (1966), Blackband (1960), Checcacci (1966), Golton and Walker (1971), Kersley and Taylor (1974), Klobuchar et al. (1968), Klobuchar and Whitney (1966), Lawrence et al. (1963), Liszka (1961, 1966), Lyon (1965, 1970), Mendillo et al. (1970), Merrill and Lawrence (1969), Münther (1966), Rao (1967), Roger (1964), Shmelovsky et al. (1963), Yeh and Swenson (1961), and Yuen and Roelofs (1966).

The Doppler method which requires that the satellite transmit at least two coherent harmonically-related frequencies has been employed by Bhonsle (1966), de Mendonça (1962), Evans and Holt (1973), Millman and Anderson (1968), and Ross (1960a, 1960b).

The combination of the Faraday and Doppler methods, often referred to as the hybrid technique, has also been successfully applied to ionospheric electron content investigations by Arendt and Soicher (1969), Burgess (1963), de Mendonça and Garriott (1962), and Golton (1962).

In this report, an evaluation is made of the accuracy of several of the analytical approaches which make use of the Faraday and Doppler phenomena for determining the ionospheric electron content. This is accomplished by means of a simulator-computer program which consists of a satellite-orbit generator, a time-variant three-dimensional electron density model and an earth magnetic field model expressed in terms of a series of spherical harmonics.

In Section II of this report, the analytical formulations for deducing the electron content in the ionosphere from Faraday and Doppler measurements are described.

A description of the simulator which is used to synthesize the Faraday and Doppler recordings of satellite signals is given in Section III.

In Section IV, the analysis of the simulated Faraday and Doppler data and the accuracy results of the various methods for electron content determination are discussed.

The conclusions of this study are presented in Section V.

SECTION II  
THEORETICAL CONSIDERATIONS

2.1 FARADAY ROTATION

2.1.1 INTRODUCTION

The amount of angular rotation,  $\Omega$  (in radians), experienced by a linearly polarized wave traversing a one-way path in the ionosphere can be represented by the function

$$\Omega = \frac{K_1}{f^2} \int_0^{h_s} H \cos \theta f(h) N_e dh \quad (2-1)$$

where  $K_1$  is a constant equal to  $2.362 \times 10^4$  cgs units,  $f$  is the transmission frequency in Hz,  $H$  is the magnetic field intensity in Gauss,  $f(h)$  is the secant of angle between the ray path and the zenith,  $N_e$  is the electron density in electrons/cm<sup>3</sup>,  $dh$  is the height differential in cm, and  $\theta$  is the propagation angle, i. e., the angle between the direction of the earth's magnetic lines of force and the direction of propagation.

This relationship which is derived in Appendix A contains only the first-order term for the refractive index. As a first approximation, the higher order terms have been neglected.

Since the combined function,  $H \cos \theta f(h)$ , varies relatively slowly with altitude (Millman and Rose, 1961), it is valid to remove the terms outside the integral of Equation (2-1).

Thus, the angular rotation can be written in the form

$$\Omega \approx \frac{K_1}{f^2} \bar{M} N_t \quad (2-2)$$

where  $\bar{M}$  is the mean value of the geometric magnetic factor

$$\bar{M} = \overline{H \cos \theta f(h)} \quad (2-3)$$

and  $N_t$  is the integrated electron density in a vertical column up to the satellite altitude,  $h_s$ ,

$$N_t = \int_0^{h_s} N_e dh \quad (2-4)$$

An alternative form for expressing Equation (2-1) is

$$\Omega \approx \frac{K_1}{f^2} \overline{H \cos \theta} N_r \quad (2-5)$$

where  $N_r$  is the integrated electron density along the ray path, i. e., oblique path,

$$N_r = \int_0^R N_e dr = \int_0^{h_s} N_e f(h) dh \approx \overline{f(h)} \int_0^{h_s} N_e dh \quad (2-6)$$

For any ray path, the parameter  $\overline{M}$  or  $\overline{H \cos \theta}$  can be readily specified. In this study, the magnetic field intensity,  $H$ , and the propagation, angle,  $\theta$ , are determined by assuming a spherical harmonic model for the earth's magnetic field. A complete description of the model is given in Appendix A.

According to Equations (2-2) and (2-5), the electron content along either a vertical or oblique path can be deduced when the Faraday polarization rotation angle,  $\Omega$ , is known.

In general, for radio waves emitted from satellites and observed on the ground, the experimentally-measured total angular rotation,  $\Omega_e$ , is ambiguous in that

$$\Omega_e = \pm (n\pi \pm \Delta \Omega) \quad (2-7)$$

where  $n$  is a positive integer and  $\Delta \Omega$  is the acute polarization angle which would normally be indicated in a satellite-amplitude measurement.

### 2.1.2 SINGLE FREQUENCY METHOD

It is possible, however, that, for transmissions in the VHF and UHF range, the polarization rotation could be less than  $(\pi/2)$  radians. This could occur under certain conditions; that is, when observations are made during the nighttime or at certain azimuth-elevation angle orientations toward the polar ionosphere (in the case of a polar orbiting satellite) where near perpendicularity with the earth's magnetic field could be attained.

Assuming that the angular rotation is initially less than  $(\pi/2)$  radians, then, when  $(\pi/2)$  radian rotation does occur, the integrated electron density, i.e., electron content, can be readily derived from Equations (2-2) or (2-5) utilizing a single transmission frequency.

In radar-lunar studies of the ionosphere by the single frequency - Faraday method, the ambiguity problem was resolved by theoretically estimating the expected angular rotation along various earth-moon paths (Millman, 1964). The measured angular rotation, as defined by Equation (2-7), that best correlated with the theoretical calculations was then selected as the parameters to be used in evaluating the integrated electron density along the ray path. In the theoretical computation of the magnitude of the Faraday rotation, the electron density distribution derived from ionosonde data was used to characterize the ionosphere up to the height of maximum ionization of the F-layer. Above the peak of the F-layer, the distribution of electron density with height was assumed to follow a Chapman model.

### 2.1.3 TWO FREQUENCY METHOD

One method for resolving the ambiguity of the complete number of polarization rotations is to employ two closely-spaced frequencies. By comparing the amplitude fading on, for example, 40 and 41 MHz, the ambiguity could be reduced to a multiple of 20 half-rotations (Blackband, 1960). Alternate approaches to the removal of the  $n\pi$  ambiguity in the Faraday rotation measurements have been proposed by Crooker (1970), Titheridge (1971), and Smith (1971).

When two harmonically-related frequencies are used, i.e.,  $mf_1 = f_2$ , it can be shown from Equation (2-2) that, when neglecting 2nd order effects, the electron content is given by

$$N_t = \frac{m^2 f_1^2}{K_1 \bar{M}} \left[ \frac{\Omega(f_1) - \Omega(f_2)}{m^2 - 1} \right] \quad (2-8)$$

### 2.1.4 DIFFERENTIAL POLARIZATION ROTATION ANGLE METHOD

The ambiguity problem can be avoided by the measurement of the change in the polarization angle at two different times,  $t_1$  and  $t_2$ , on the satellite orbit pass. This scheme which is often referred to as the differential Faraday polarization rotation angle method requires that the integrated electron densities along the two different ray paths be identical.

This assumption implies that no horizontal gradients of electron content exist within the time interval. Thus, it can be shown from Equation (2-2) that the electron content can be obtained from

$$N_t = \frac{f^2}{K_1} \left[ \frac{\Omega_1 - \Omega_2}{M_1 - M_2} \right] \quad (2-9)$$

#### 2.1.5 POLARIZATION ROTATION RATE METHOD

Another method which can be used to determine  $N_t$  is one which involves the time rate of change of the polarization rotation angle. Differentiating Equation (2-2) with respect to time results in

$$\dot{\Omega} = \frac{K_1}{f^2} \left[ \bar{M} \dot{N}_t + N_t \dot{\bar{M}} \right] \quad (2-10)$$

where the dot signifies the time derivative.

Assuming a horizontally stratified ionosphere, then  $\dot{N}_t = 0$ . It follows that

$$N_t = \frac{f^2}{K_1} \frac{\dot{\Omega}}{\dot{\bar{M}}} \quad (2-11)$$

The electron content can therefore be determined since  $\Omega$  can be experimentally measured and  $\dot{\bar{M}}$  theoretically predicted.

A more sophisticated technique which eliminates the restriction of no horizontal gradients requires the 2nd derivative of  $\Omega$  which, according to Equation (2-9), evaluates to

$$\ddot{\Omega} = \frac{K_1}{f^2} \left[ \bar{M} \ddot{N}_t + 2 \dot{\bar{M}} \dot{N}_t + N_t \ddot{\bar{M}} \right] \quad (2-12)$$

If it is assumed that  $N_t$  is of the form

$$N_t = a + bt \quad (2-13)$$

then  $\ddot{N}_t = 0$ . It follows from Equations (2-10) and (2-12) that the electron content can be expressed by

$$N_t = \frac{f^2}{K_1} \left[ \frac{\overline{M} \ddot{\Omega} - 2 \dot{\overline{M}} \dot{\Omega}}{\overline{M} \ddot{\overline{M}} - 2 \dot{\overline{M}}^2} \right] \quad (2-14)$$

#### 2.1.6 LEAST SQUARE METHOD

This method which was proposed by Burgess (1963) and evaluated by Garriott and de Mendonça (1963) involves the assumption that the electron content can be represented by a power series

$$N_t = a + bt + ct^2 + \dots \quad (2-15)$$

At  $t = 0$ , which corresponds to the time of the satellite point of closest approach,  $(N_t)_0 = a$  and Equation (2-2) becomes

$$\Omega_0 = A \overline{M}_0 (N_t)_0 = A \overline{M}_0 a \quad (2-16)$$

where  $A = (K_1/f^2)$ .

With the use of Equations (2-15) and (2-16), Equation (2-2) can be written as

$$\Omega - \Omega_0 = Aa (\overline{M} - \overline{M}_0) + Ab \overline{M} t + Ac \overline{M} t^2 + \dots \quad (2-17)$$

It is noted that the Faraday rotation angle at two different times,  $\Omega - \Omega_0$ , can be readily determined from the experimental data.

The least square error,  $\epsilon$ , can then be evaluated from

$$\epsilon = \frac{1}{n} \sum_1^n \left[ (\Omega - \Omega_0) - Aa (\overline{M} - \overline{M}_0) - Ab \overline{M} t - Ac \overline{M} t^2 - \dots \right]^2 \quad (2-18)$$

where  $n$  is the number of observations.

Minimizing  $\epsilon$  with respect to the coefficients,  $a$ ,  $b$ ,  $c$ , etc.,

$$\frac{\partial \epsilon}{\partial a} = \frac{\partial \epsilon}{\partial b} = \frac{\partial \epsilon}{\partial c} = \dots = 0 \quad (2-19)$$

results in a set of linear equations. The coefficients can then be evaluated from the simultaneous solution of the linear equations.

A method of solution of the linear equations has been proposed by Garriott and de Mendonça (1963).

## 2.2 DIFFERENTIAL PHASE AND DOPPLER FREQUENCY SHIFT

### 2.2.1 INTRODUCTION

The differential phase or dispersive phase method can be considered to be a modified form of the Doppler frequency technique.

The differential phase between two harmonically-related coherent signals transmitted from a satellite and detected on the ground is given by

$$\Delta\phi = -\frac{K_2}{f_1} \left( \frac{b^2 - a^2}{a} \right) N_r \quad (2-20)$$

where  $K_2$  is a constant equal to  $8.440 \times 10^{-3}$  cgs units, and  $a$  and  $b$  are constants related to the satellite transmitted frequencies,  $f_1$  and  $f_2$ , according to

$$af_1 = bf_2 \quad (2-21)$$

It is noted that differential phase between the two frequencies is obtained from

$$\Delta\phi = a\phi_1 - b\phi_2 \quad (2-22)$$

where  $\phi_1$  and  $\phi_2$  are the total phase shifts encountered by the radio waves traversing a space-to-earth propagation path.

Equation (2-20), which is derived in Appendix B, is based on the assumption that the two transmitted signals travel along the same ray path and that higher order terms of the refractive index can be neglected.

The differential phase can also be written as

$$\Delta\phi = -\frac{K_2}{f_1} \left( \frac{b^2 - a^2}{a} \right) \overline{f(h)} N_t \quad (2-23)$$

where  $\overline{f(h)}$  is the mean value of the geometric function,  $f(h)$ , and where, as indicated by Equation (2-6),

$$N_r \approx \overline{f(h)} N_t \quad (2-24)$$

The absolute phase of a satellite signal received on the ground cannot be measured. Thus, from the differential phase, Equation (2-20), the relative electron content along the paths from the satellite to a ground terminal throughout the satellite pass can only be inferred.

### 2.2.2 DOPPLER FREQUENCY SHIFT METHOD

An absolute measure of the electron content can be determined from the Doppler frequency shifts of the coherent transmissions from a satellite. According to Al'pert (1958), for a satellite moving in a circular orbit and assuming that the ionosphere is nonrefractive and fixed in configuration, both in time and space, the ionospheric electron content in a vertical column can be evaluated from

$$\int_0^{h_s} N_e dh = \frac{h_s f_1^2}{K_3} \left( f_{d2} - f_{d1} \frac{f_2}{f_1} \right) \left( f_{d2} - f_{d1} \frac{f_1}{f_2} \right)^{-1} \quad (2-25)$$

where  $K_3$  is a constant equal to  $4.03 \times 10^7$  cgs units,  $h_s$  is the satellite altitude and  $f_{d1}$  and  $f_{d2}$  are the Doppler frequency shifts of the satellite emitted frequencies,  $f_1$  and  $f_2$ , respectively. This expression is valid for satellites located at high elevation angles with respect to the ground receiving station.

As shown in Appendix B, the Doppler frequency shift of satellite signals traversing the ionosphere can be expressed by

$$f_d = -\frac{f}{c} \dot{R} + \frac{K_4}{f} \frac{d}{dt} \int_0^R N_e dr \quad (2-26)$$

where  $K_4$  equals  $1.343 \times 10^{-3}$  cgs units and  $\dot{R}$  is the radial velocity of the satellite. This equation is derived on the basis of using only first-order approximations for the index of refraction.

Once the integrated electron density is known for one point on the satellite trajectory, it is then possible to convert the relative electron content scale, as deduced from differential phase as defined by Equation (2-23), into an absolute measurement. Thus, the electron content in a slant column can be derived for all points on the satellite orbit from Equation (2-24).

### 2.2.3 DOPPLER FREQUENCY SLOPE METHOD

A modification of Al'pert's expression for calculating the integrated electron density is the Doppler slope method described by Arendt et al. (1965). According to Arendt et al. (1965), when the satellite is at the point of closest approach, the columnar electron content can be represented by

$$\int_0^{h_s} N_e dh = \frac{h_s f_1^2}{K_3} \left( \sigma_2 - \sigma_1 \frac{f_2}{f_1} \right) \left( \sigma_2 - \sigma_1 \frac{f_1}{f_2} \right)^{-1} \quad (2-27)$$

where  $\sigma_1$  and  $\sigma_2$  are the Doppler slopes at the inflection points for the frequencies  $f_1$  and  $f_2$ , respectively.

It should be noted that this relationship closely resembles Equation (2-25) derived by Al'pert (1958). The criterion for applying the Doppler slope method has been discussed by Arendt (1966). In essence, the criterion for a minimum prerequisite for the applicability of the Doppler method is given by the inequality

$$0 < \frac{f_{d1}}{f_{d2}} \frac{f_2}{f_1} < 1 \quad (2-28)$$

### 2.2.4 IONOSONDE METHOD

The ionosonde method which was suggested by Evans and Holt (1973) for the calibration of the differential phase records utilizes the concept that the electron density distribution in the ionosphere can be represented by the Chapman model of the form

$$N_e = N_m \exp \frac{1}{2} \left\{ 1 - \frac{(h - h_m)}{H_s} - \exp \left[ - \frac{(h - h_m)}{H_s} \right] \right\} \quad (2-29)$$

where  $H_s$  is the scale height of the neutral particles (atomic oxygen) and  $N_m$  is the electron density at the level of maximum ionization,  $h_m$ .

The maximum electron density of the layer is obtained by the use of a vertical incidence ionospheric sounder and is related to the ordinary wave - critical frequency of the F-layer,  $f_o F2$ , by

$$N_m = \frac{\pi m_e}{e^2} (f_o F2)^2 = 1.241 \times 10^{-8} (f_o F2)^2 \quad (2-30)$$

where  $N_m$  is in electrons/cm<sup>3</sup>,  $m_e$  is the electron mass,  $e$  is the electron charge and  $f_o F2$  is in Hz.

The scale height of the layer (in km) is defined in terms of

$$H_s = 63.15 + 6.29 \sin \left[ \frac{(h - 9) \pi}{12} \right] + 17.66 \sin \left[ \frac{(D - 60) \pi}{183} \right] \quad (2-31)$$

where  $h$  is the local time in hours and  $D$  is the day of the year.

This analytical model was derived by Klobuchar and Allen (1970) from total electron content data deduced from Faraday rotation measurements of radio wave transmissions from the ATS-3 geostationary satellite. The observations were conducted at the AFCRL Sagamore Hill Radio Observatory, Hamilton, Massachusetts, (geographic coordinates: 42.6°N, 70.8°W).

In order to employ the Chapman distribution, the height of the F-layer maximum must be known. From incoherent scatter observations made at the Millstone Hill radar facility, Westford, Massachusetts, (geographic coordinates: 42.6°N, 71.5°W), Evans and Holt (1973) have concluded that  $h_m$  (in km) can be represented by the function

$$h_m = 280 + 40 \cos \left[ \frac{(h + 1) \pi}{12} \right] \quad (2-32)$$

When the three parameters,  $N_m$ ,  $H_s$  and  $h_m$  are available, it is then possible to integrate Equation (2-29) to obtain the integrated electron density in a vertical column to the satellite altitude. Assuming no horizontal gradients of electron density, the electron content in an oblique path can then be computed from Equation (2-6).

Wright (1960) has shown that, if the electron density distribution in the ionosphere is of the Chapman form, the total integrated electron density can be expressed in terms of the scale height and the maximum electron density by

$$\int_0^{\infty} N_e dh = 4.133 N_m H_s \quad (2-33)$$

It follows from Equation (2-30) that the electron content can be determined from the F-layer critical frequency by

$$N_t = 5.129 \times 10^8 (f_o F2)^2 H_s \quad (2-34)$$

It should be noted that, according to Equations (2-33) and (2-34), the maximum electron density or the critical frequency of the F-layer, in addition to the scale height, can be used to compute the electron content. However, this procedure is valid for satellites at geostationary altitudes or at approximately 2 to 3 earth radii from the ground. For TRANSIT satellites which orbit the earth in the vicinity of 1000 km altitude, it is necessary to integrate Equation (2-29) to the satellite altitude for electron content determination.

#### 2.2.5 LEAST SQUARE METHOD

This method, which is similar to the one used for the analysis of Faraday rotation data, was also proposed by Burgess (1963).

Expressing the electron content,  $N_t$ , as a power series in time, Equation (2-15), then, at  $t = 0$ , which corresponds to the time when  $\Delta\dot{\phi} = 0$ ,  $(N_t)_0 = a$  and Equation (2-23) becomes

$$\Delta\phi_0 = B \overline{f(h)_0} (N_t)_0 = B \overline{f(h)_0} a \quad (2-35)$$

where

$$B = - \frac{K_2}{f_1} \left( \frac{b^2 - a^2}{a} \right) \quad (2-36)$$

Thus, it can be shown, utilizing Equations (2-15), (2-23), and (2-35), that the differential phase at two different times,  $\Delta\phi - \Delta\phi_0$ , which is measurable, can be written as

$$\Delta\phi - \Delta\phi_0 = Ba \left[ \overline{f(h)} - \overline{f(h)}_0 \right] + Bb \overline{f(h)}t + Bc \overline{f(h)} t^2 + \dots \quad (2-37)$$

The least square error therefore becomes

$$\epsilon = \frac{1}{n} \sum_1^n \left[ (\Delta\phi - \Delta\phi_0) - Ba \left( \overline{f(h)} - \overline{f(h)}_0 \right) - Bb \overline{f(h)} t - Bc \overline{f(h)} t^2 - \dots \right] \quad (2-38)$$

The simultaneous solution of the set of linear equations obtained where  $\epsilon$  is minimized, with respect to  $a$ ,  $b$ ,  $c$ , etc., will result in an evaluation of the coefficients.

A least square method which assumes that the electron content varies linearly with time has been considered by de Mendonça (1962).

### 2.3 FARADAY ROTATION - DIFFERENTIAL DOPPLER

The combination of the Faraday rotation and differential Doppler technique to determine the ionospheric electron content was originally suggested by Burgess (1962).

The mathematical formulation of this technique can be readily derived by differentiating Equations (2-5) and (2-20) with respect to time. Hence, there results

$$\dot{\Omega} = \frac{K_1}{f_1^2} \left[ \overline{H \cos \theta} \dot{N}_r + N_r \overline{H \cos \theta} \right] \quad (2-39)$$

$$\Delta\dot{\phi} = - \frac{K_2}{f_1} \left( \frac{b^2 - a^2}{a} \right) \dot{N}_r \quad (2-40)$$

Combining the two expressions,  $N_r$  can be readily solved from

$$N_r = \frac{1}{\overline{H \cos \theta}} \left[ \frac{\dot{\Omega} f_1^2}{K_1} - 2\pi \overline{H \cos \theta} \frac{f_1}{K_2} \left( \frac{a}{b^2 - a^2} \right) \Delta f_d \right] \quad (2-41)$$

where  $\Delta f_d$  is the differential Doppler frequency shift

$$\Delta f_d = - \frac{1}{2\pi} \Delta\dot{\phi} \quad (2-42)$$

When  $\Delta f_d = 0$ , Equation (2-41) simplifies to

$$(N_{r'o}) = \frac{1}{H \cos \theta} \frac{f_1^2}{K_1} \dot{\Omega} \quad (2-43)$$

It should be noted that this method does not require an assumption on horizontal gradients or restricting the satellite to a circular orbit, i.e., no vertical velocity component.

The Burgess hybrid Faraday-Doppler method has been modified by Golton (1962) and de Mendonça and Garriott (1962).

### SECTION III

#### COMPUTER SIMULATION OF SATELLITE TRANSMISSIONS

The accuracy of the various analytical techniques for determining the electron content in the ionosphere is evaluated by means of a simulation-computer program. The simulator basically synthesizes the Faraday and Doppler recordings of satellite signals that would be received on the ground.

The logic block diagram of the simulator is illustrated in Figure 3-1.

In the satellite-orbit generator, the azimuth angle (A), elevation angle (E), altitude (h), range (R) and range rate ( $\dot{R}$ ) of the satellite as observed as a function of time at a ground-receiving station are computed. The calculations are based on Kepler's equations of motion, i.e., a two-body orbit, assuming a rotating-spherical earth which is void of an atmosphere. The required inputs to the program are the geographical coordinates and altitude of the ground station and the satellite-orbital parameters which consist of the three orientation elements, inclination angle, argument of perigee and longitude of ascending node and the three dimensional elements, semimajor axis, eccentricity and time of ascending node.

The earth's magnetic field is represented by a series of spherical harmonics. In this analysis, the set of 80 spherical harmonic coefficients for Epoch 1965 derived by the International Association of Geomagnetism and Aeronomy (IAGA) Commission 2 Working Group 4, Analysis of the Geomagnetic Field (1969), is used to specify the magnetic potential function. This function in turn is employed in the computation of the magnetic field intensity, H, the inclination angle, I, and the declination angle, D, as discussed in Appendix A. The magnetic field intensity and the propagation angle,  $\theta$ , which is a function of I and D, are evaluated at equal increments of height along the different propagation paths to the orbiting satellite.

The electron density profiles generated by the Penn State Mark I Ionospheric Model (Nisbet, 1970) are used as the reference ionosphere. However, the simulator can also accept as an input any spatial distribution of electron density. The required inputs to the model are geographic coordinates, day number, time of day and solar activity, i.e., 10.7 cm solar flux intensity. The output of the model is in the form of hourly values of the electron density profile [  $N_e(h)$  ], between 120- and 1250-km altitude.

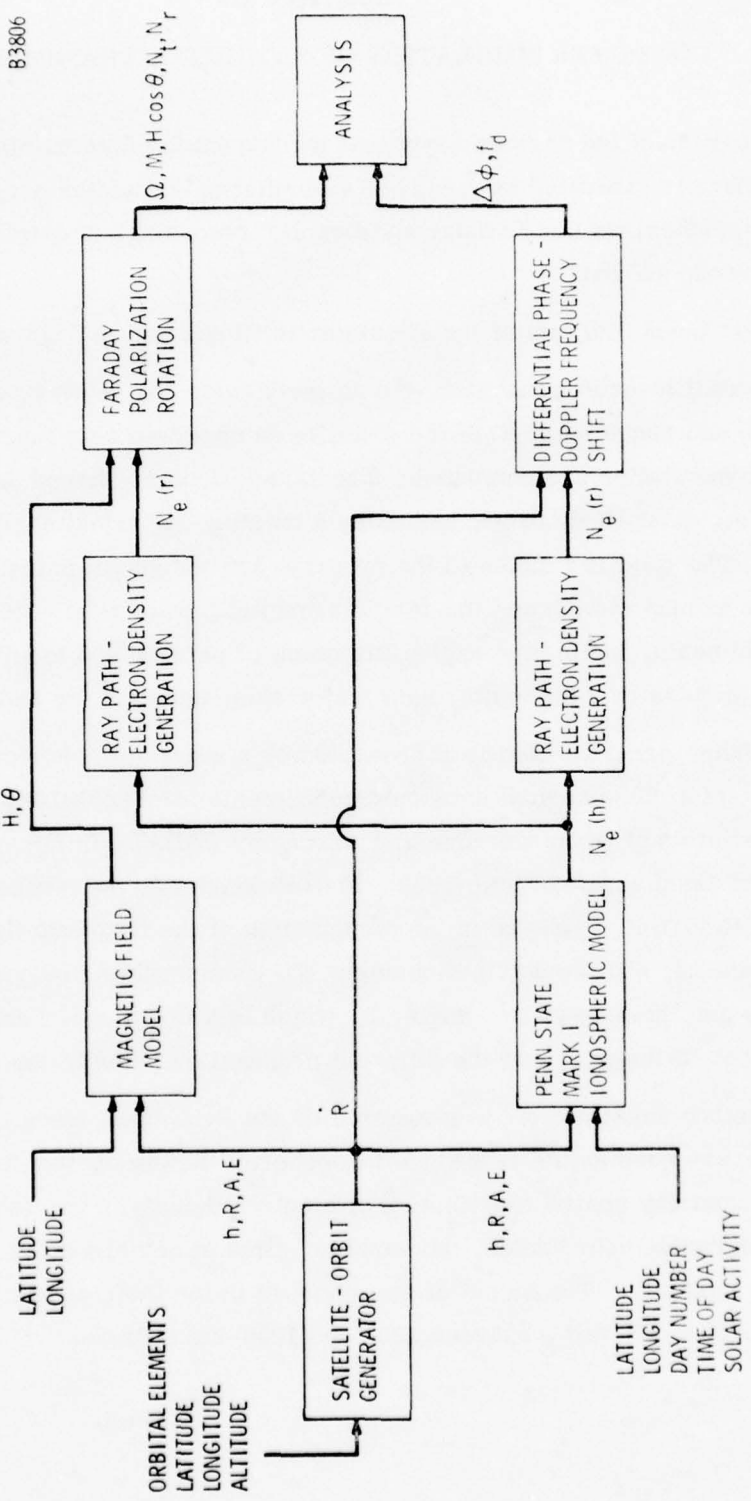


Figure 3-1. Logic Block Diagram of Faraday-Doppler Simulator

The spatial distribution of electron density is attained by generating vertical profiles at three locations north of the satellite-observing site and three locations south of the site, each separated by  $10^\circ$  geographic latitude. The data for the six additional locations yield latitudinal-electron density coverage and information on the existence of north-south electron density gradients. Since the hourly values of the electron density profiles can be converted directly to  $15^\circ$  longitudinal values, the east-west gradients are also available.

In the ray path - electron density generator, the electron densities along the different ray paths,  $[N_e(r)]$ , are determined by linear interpolation within the vertical distribution - electron density grid.

In the Faraday rotation module, the first-order term of the polarization rotation angle ( $\Omega$ ) is calculated at even height increments along the ray path. The output data also consist of the geometric magnetic factor ( $M$ ), the magnetic function ( $H \cos \theta$ ), the integrated electron density in a vertical column ( $N_t$ ) and along an oblique path ( $N_r$ ).

The differential phase between the two coherent transmitted satellite frequencies ( $\Delta\phi$ ) is calculated along the path to the satellite. In addition, the Doppler frequency shift ( $f_d$ ) experienced by the two frequencies is also determined. In both derivations, the first-order refractive index term is only used.

The output data from the Faraday rotation and differential phase-Doppler shift modules which in reality can be considered to be a ground-satellite receiving system is processed in the analysis program. The analytical techniques for ionospheric electron content determination that are evaluated are the Faraday single frequency method, differential polarization rotation angle method, polarization rotation rate method, Doppler frequency shift method, Doppler frequency slope method, ionosonde method and the hybrid Faraday rotation-differential Doppler method.

The electron contents deduced by the analytical techniques are compared with the true-reference values obtained by integration of the ray paths - electron densities in the Faraday rotation module.

SECTION IV  
SIMULATOR - DATA ANALYSIS

The simulated Faraday rotation, differential phase and Doppler data presented in this report are derived on the premise that the 150- and 400-MHz transmissions from the TRANSIT satellite, Object No. 1970-067A, are recorded at the General Electric Radio-Optical Observatory, located at 42.85°N latitude and 74.07W longitude (54.3°N geomagnetic latitude) near Schenectady, New York. The satellite which was launched on August 27, 1970 is in a polar orbit with an inclination of approximately 90°, apogee of 1219 km, perigee of 956 km and period of 106.9 minutes.

The earth trace of the satellite orbit at approximately 1800 hours GMT on June 3, 1974, is shown in Figure 4-1 together with the geographic coordinates of the locations where the electron density - height profiles are generated utilizing the Penn State Ionospheric model.

The altitude and azimuth-elevation angles of the satellite orbit as predicted for Schenectady, New York, are plotted in Figure 4-2. The azimuth and maximum elevation angle corresponding to the point of closest approach is 276.2° and 71.8°, respectively. The orbit calculations are based on the assumption that a vacuum exists between the ground station and the satellite. In other words, tropospheric and ionospheric refraction and time delay effects are neglected. The decrease in satellite altitude from 1200 to 1083 km during the orbital pass is indicative of the fact that the satellite has a velocity component in the vertical direction. In the evaluation of the various analytical techniques discussed in this report, it is assumed that the satellite is travelling in a circular orbit, i. e., vertical velocity component is neglected.

The vertical distributions of electron density along the 74.07°W meridian at 1800 hours GMT are illustrated in Figure 4-3. The profiles pertain to the seven locations each separated by 10° geographic latitude. The center profile corresponds to the receiver site at Schenectady, New York.

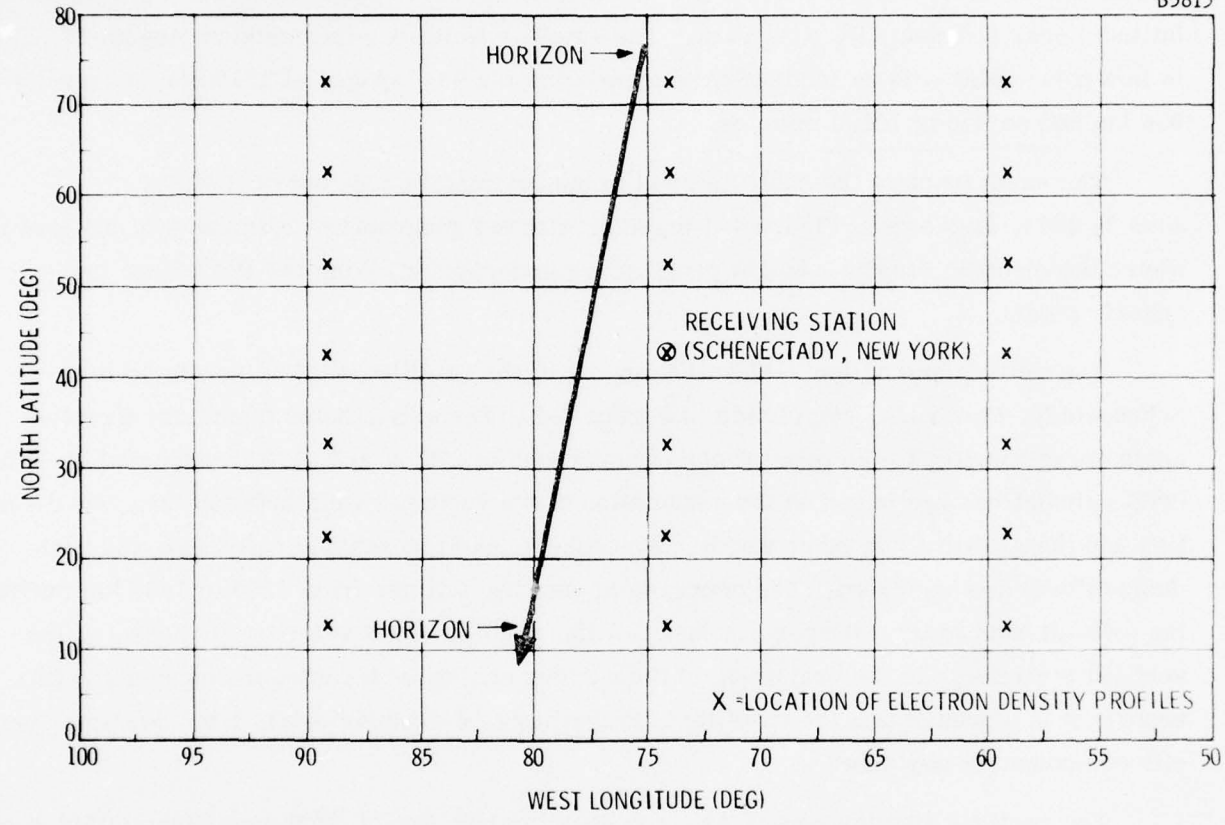


Figure 4-1. Earth Trace of the Orbit of TRANSIT Satellite, Object No. 1970-067A, June 3, 1974 and Geographic Coordinate - Location of Vertical Distributions of Electron Density

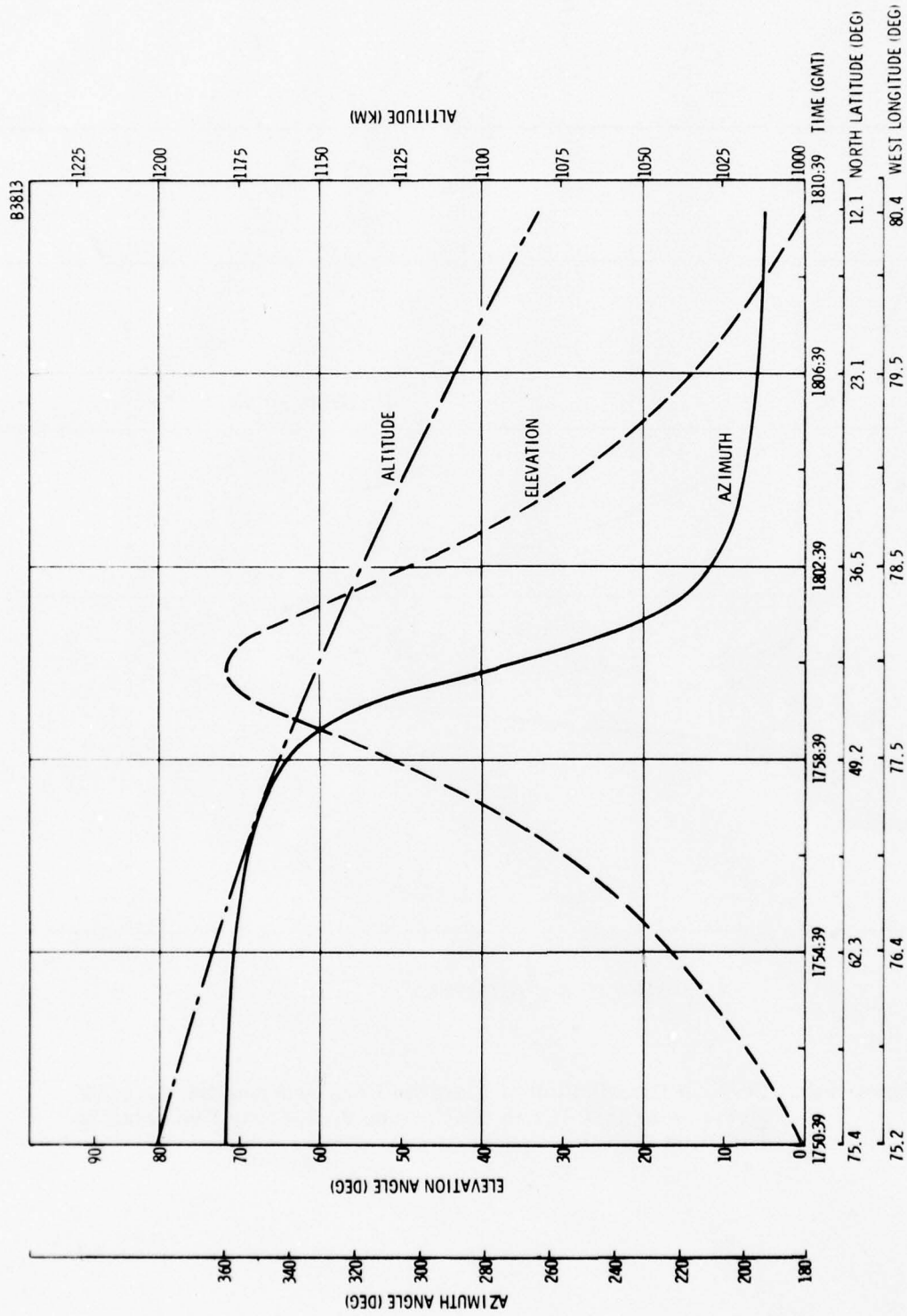


Figure 4-2. Altitude and Angular Coordinates of TRANSIT Satellite, Object No. 1970-067A, June 3, 1974, as Predicted for Schenectady, New York

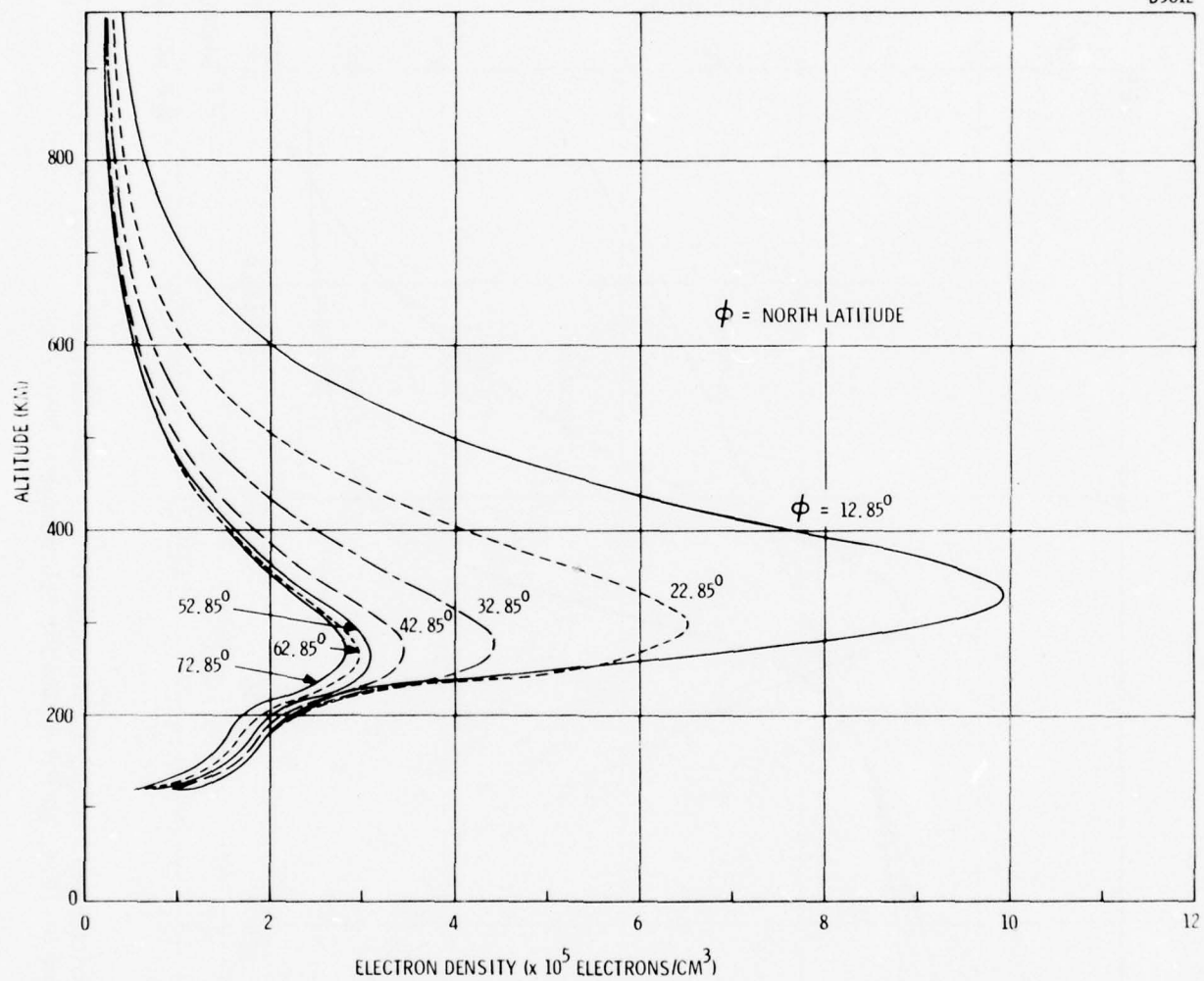


Figure 4-3. Vertical Distribution of Electron Density Along the 74.07°W Meridian at 1800 Hours GMT, June 3, 1974 As Predicted by The Penn State Ionosphere Model

It is evident that the height and maximum ionization level of the F-layer peak is latitude dependent. That is, the electron density and layer height are a maximum in the southern latitudes and a minimum in the northern latitudes. In the vicinity of Schenectady, the F-layer peak is at an altitude of approximately 270 km.

The latitude dependency of electron density signifies the presence of an ionization gradient. The gradient is apparent in Figure 4-4 which depicts the integrated electron density in a vertical and slant (oblique) column to the satellite altitude and along the satellite azimuth - elevation direction.

The simulated Faraday polarization rotation angles of the 150- and 400-MHz signals from the TRANSIT satellite are plotted in Figure 4-5. It should be noted that the satellite was designed to transmit circular polarization but, on a reception at the ground, the polarization is degraded somewhat to elliptical because of the geometric orientation of the satellite antenna with respect to a ground receiving antenna. For this analysis, it is assumed that the TRANSIT satellite radiates linear polarization. The ambiguous curves are representative of the data that would be experimentally observed while the unambiguous curves are the theoretical estimates of the total rotation that the two frequencies would encounter in traversing the ionosphere. As a result of magnetic field geometry, minimum angular rotation is attained at an azimuth angle of  $358.2^\circ$  and elevation angle of  $9.3^\circ$ .

In evaluating the single-frequency Faraday rotation method, it is appropriate to consider only the 400-MHz data in order to insure the occurrence of minimum-angular polarization rotation, and thus avoid the ambiguity problem.

According to Figure 4-5, the ambiguous angular rotation of the 400-MHz transmission is less than  $\pi$  radians. The geometric magnetic factor,  $M$ , and the magnetic function,  $H \cos \theta$ , at  $193.5^\circ$  azimuth and  $9.1^\circ$  elevation, which corresponds to the direction of the  $(\pi/2)$  radian angular rotation, are plotted in Figure 4-6.

Utilizing Equations (2-2) and (2-5), the electron content along a vertical path,  $N_t$ , and along a slant path,  $N_r$ , can be readily deduced for a given angular rotation,  $\Omega$ .

Figure 4-7 depicts the error in determining the vertical and the slant electron content in the direction of ambiguous Faraday rotation  $(\pi/2)$  radians at 400 MHz. The error,  $\Delta N_{r,t}$ , is evaluated from the expression

$$\Delta N_{r,t} = \frac{N_{r,t} - N'_{r,t}}{N'_{r,t}} \quad (4-1)$$

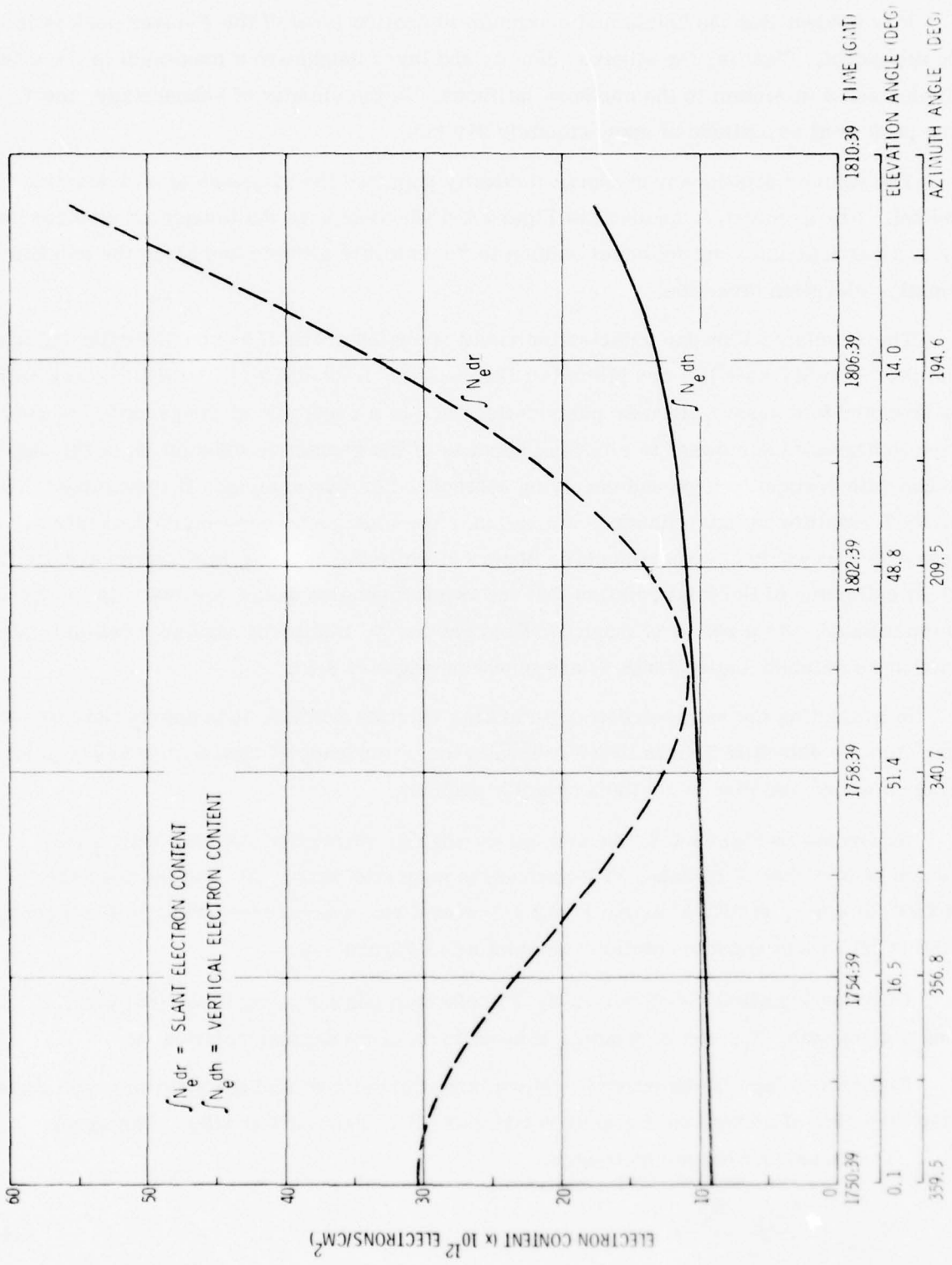


Figure 4-4. Electron Content on June 3, 1974, As Predicted By The Penn State Ionosphere Model

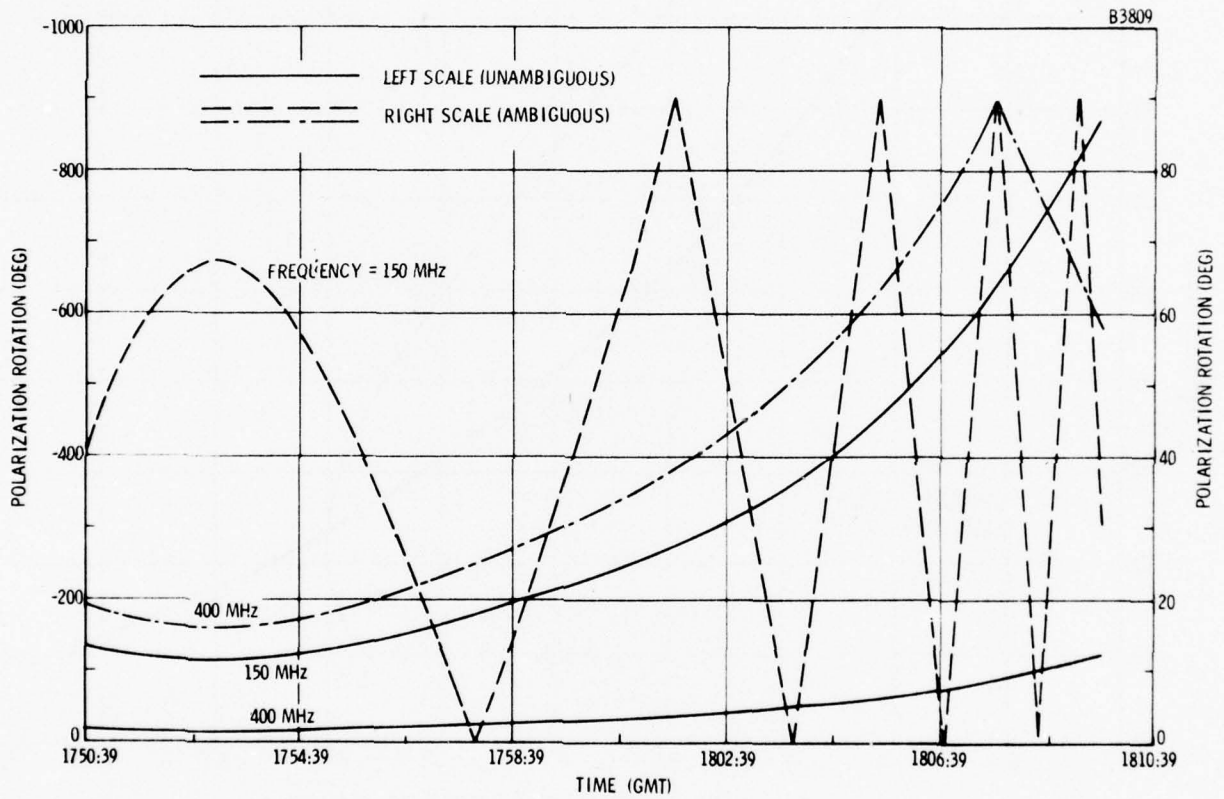


Figure 4-5. Simulated Faraday Polarization Rotation Angle of TRANSIT Satellite, Object No. 1970-067A, June 3, 1974

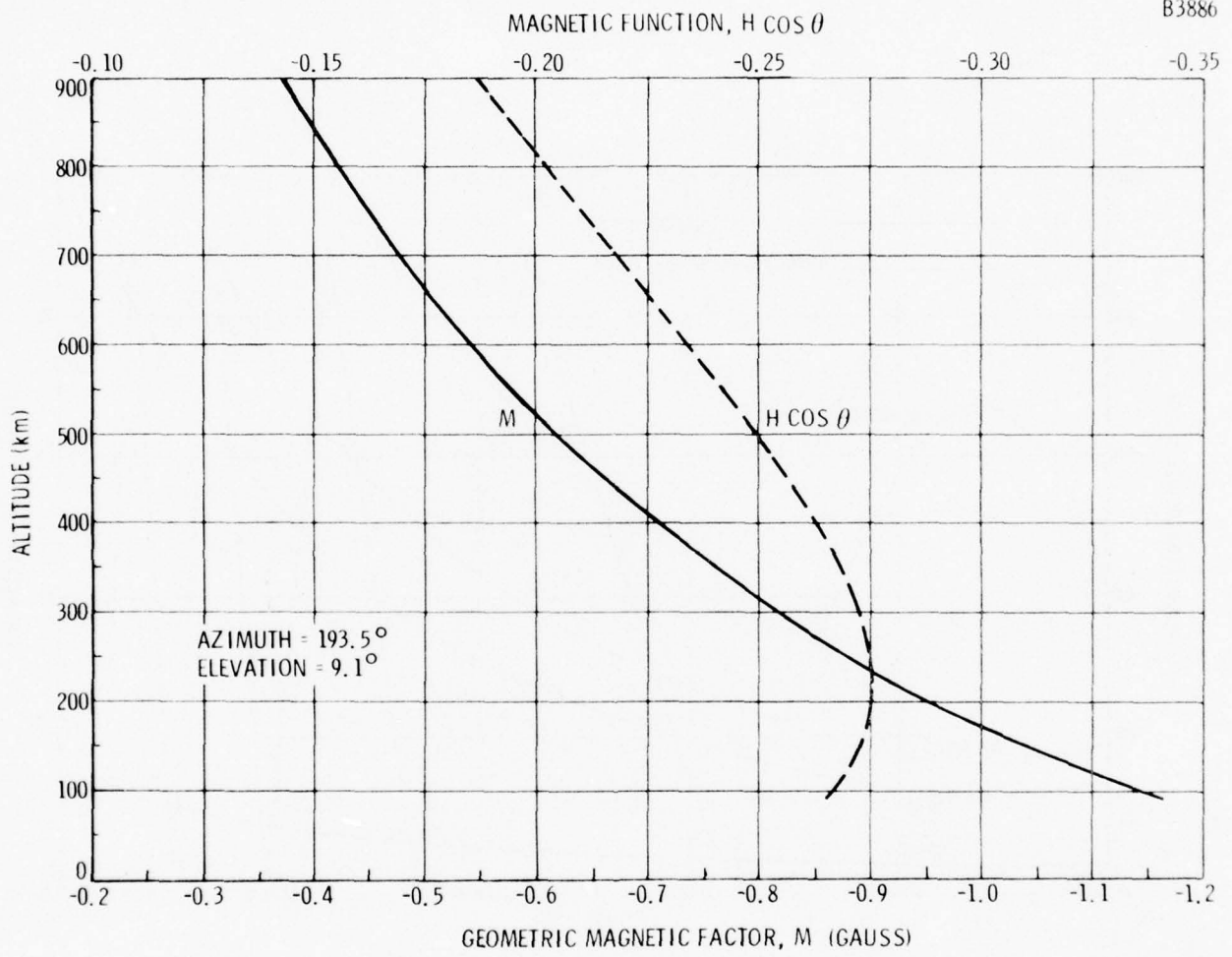


Figure 4-6. The Parameters M and H cos  $\theta$  in the Direction of Ambiguous Faraday Rotation of  $\pi/2$  Radians at 400 MHz

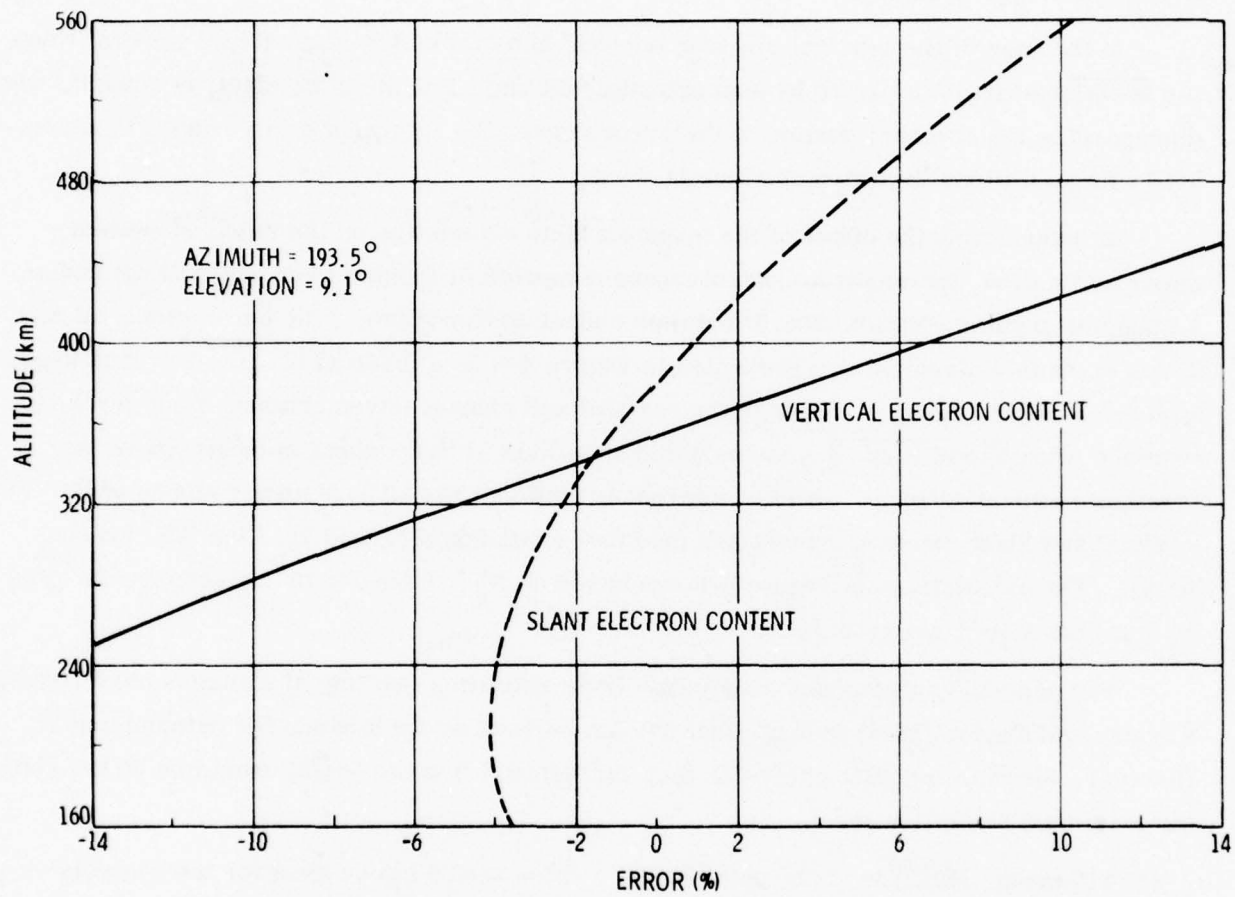


Figure 4-7. Error in Determining the Vertical and Slant Electron Content in the Direction of Ambiguous Faraday Rotation of  $\pi/2$  Radians at 400 MHz By the Single Frequency Method

where the prime signifies the theoretical prediction. For this example,  $N_r' = 4.0221 \times 10^{13}$  electrons/cm<sup>2</sup> and  $N_t' = 1.4050 \times 10^{13}$  electrons/cm<sup>2</sup>. It is seen that zero error exists for the vertical electron content when the value of the  $\overline{M}$  factor at an altitude of 354 km is used. However, for the slant electron content, the altitude for the  $\overline{H \cos \theta}$  value is increased to 380 km. It is noted that, in the  $(\pi/2)$  radian direction, the peak of the maximum ionization, is located at approximately 280 km altitude.

In the case of the vertical electron content, the error is increased by 1 percent when the  $\overline{M}$ -value altitude is varied by approximately 14 km. For the slant electron content, when disregarding the reversal portion of the error curve, the 1 percent error change is associated with an altitude deviation of about 14.5 km.

In determining the effect of the magnetic field orientation on the electron content - error estimation, the electron contents were computed in the direction of the  $(\pi/4)$  radian - ambiguous angular rotation (206.5° azimuth and 44.5° elevation). The parameters,  $M$  and  $H \cos \theta$ , in this direction are presented in Figure 4-8 as a function of altitude. It is apparent from Figure 4-9 that, for both the vertical and slant electron content, zero error is obtained when  $\overline{M}$  and  $\overline{H \cos \theta}$  are evaluated at 360 km altitude which is 90 km above the maximum ionization level. It is of interest to note that the altitude-error slopes of the vertical and slant electron content are modified to 10.6 km/1% and 12.1 km/1%, respectively. The calculations in Figure 4-9 are based on  $N_r' = 1.5086 \times 10^{13}$  electrons/cm<sup>2</sup> and  $N_t' = 1.1125 \times 10^{13}$  electrons/cm<sup>2</sup>.

For general analysis of Faraday data from satellites orbiting at altitudes near 1000 km, Kersley and Taylor (1974) indicate that 375 km be used as the altitude for determining  $\overline{M}$ . However, for more precise analysis, they recommend that the height should be 80 km above the maximum ionization level.

Titheridge (1972) is of the opinion that a value of 420 km be used for the analysis of geostationary satellite-Faraday rotation data and that an accuracy of  $\pm 5$  percent in electron content estimation can be expected. Klobuchar and Allen (1970), on the other hand, assumed a constant mean ionospheric height of 350 km.

According to Yeh (1974), the optimum altitude for the  $\overline{H \cos \theta}$  value in deducing the slant electron content from geostationary satellites is 680 km.

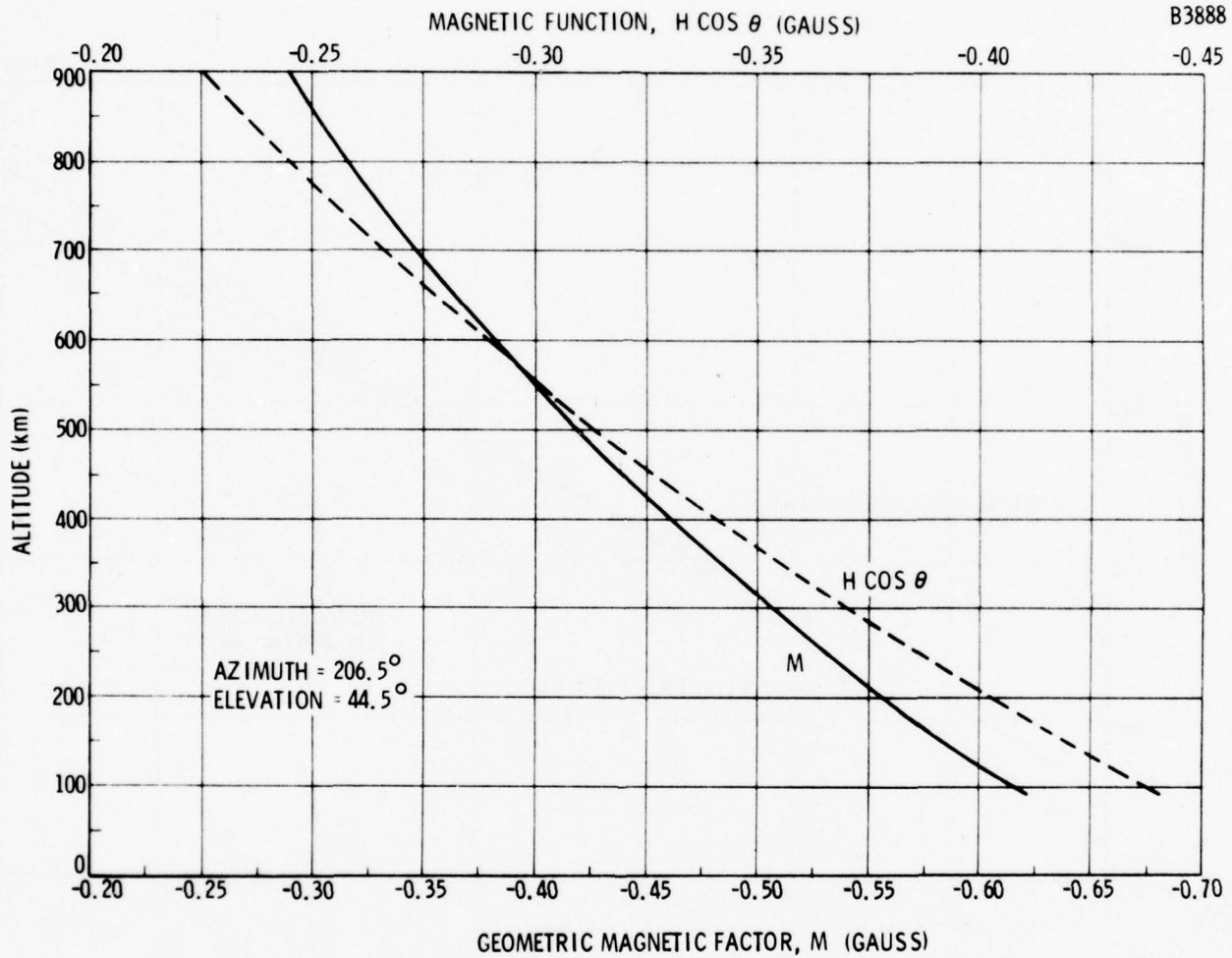


Figure 4-8. The Parameters M and  $H \cos \theta$  in the Direction of Ambiguous Faraday Rotation of  $\pi/4$  Radians at 400 MHz

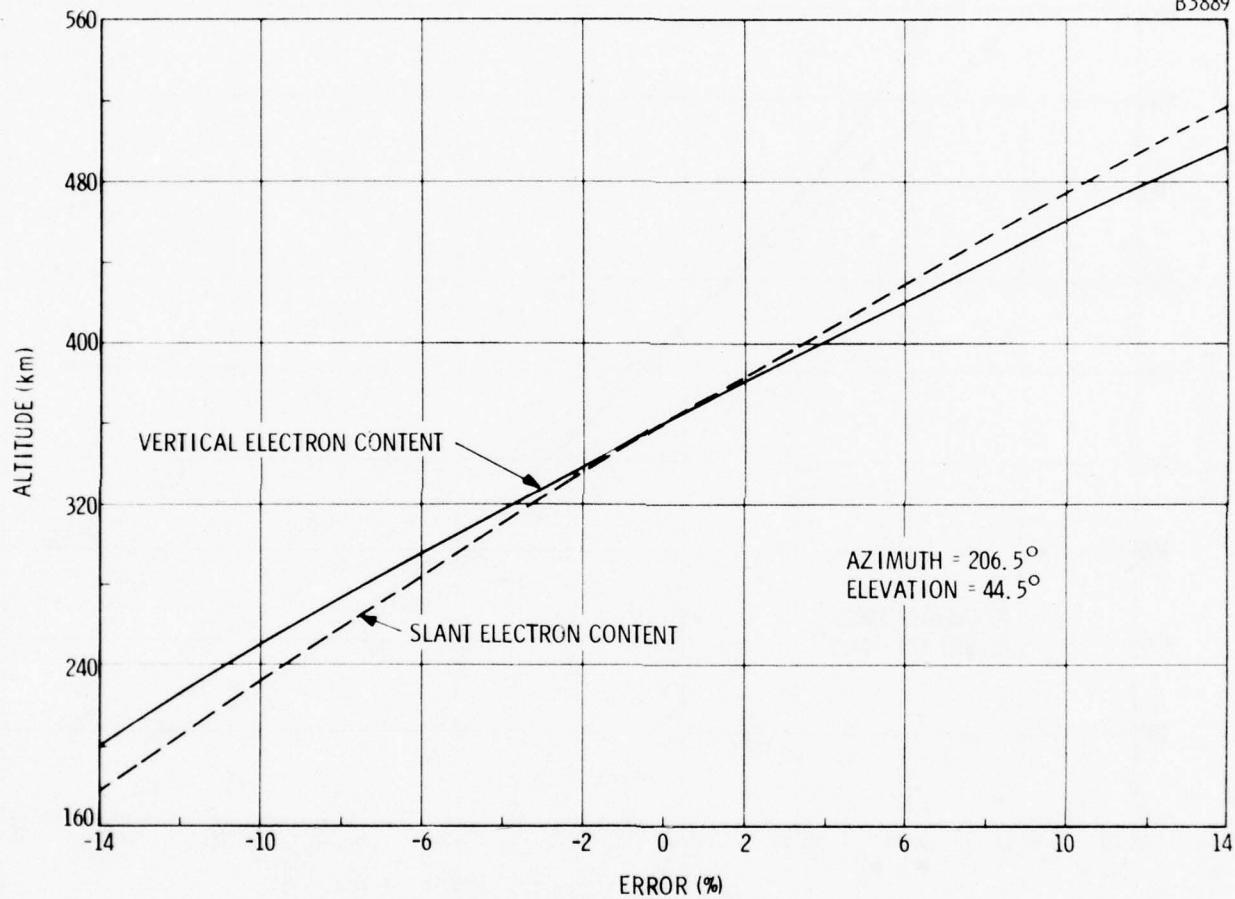


Figure 4-9. Error in Determining the Vertical and Slant Electron Content in the Direction of Ambiguous Faraday Rotation of  $\pi/4$  Radians at 400 MHz By the Single Frequency Method

The accuracy in measuring the polarization rotation angle is considered to be on the order  $\pm 5^\circ$ . Thus, for an angular rotation of  $(\pi/4)$  and  $(\pi/2)$  radians, this implies an additional error of approximately 11.1 and 5.6 percent, respectively, in resolving the electron content.

In order to minimize the effects of ionization gradients on the accuracy of the differential polarization rotation angle method, it is preferable to employ the lower frequency to deduce the electron content from the Faraday data. Since the Faraday rotation is inversely proportional to the frequency squared, as indicated by Equation (2-1), a greater number of angular rotations occurs at the lower frequency. Thus, for a given polarization twist, this permits the two locations on the satellite orbital pass, as specified by Equation (2-9), to be spatially closer together.

Although Equation (2-9) expresses the relationship for determining the vertical electron content, the slant electron content can also be readily derived by merely replacing the  $\overline{M}$  factor by the corresponding  $\overline{H \cos \theta}$  terms.

The  $M$  and  $H \cos \theta$  parameters along the ray paths in the direction of Faraday rotation difference of  $(\pi/2)$  radians at 150 MHz are plotted in Figure 4-10. These data were applied to Equation (2-9) to obtain the simulated - computed electron contents. Along both ray paths, the altitude of the maximum electron density was located at approximately 270 km. At an azimuth angle of  $346.7^\circ$  and elevation angle of  $43.0^\circ$ , the true vertical ( $N_t'$ ) and slant electron content ( $N_r'$ ) were  $1.0055 \times 10^{13}$  and  $1.3939 \times 10^{13}$  electrons/cm<sup>2</sup>, respectively, while at  $227.0^\circ$  azimuth and  $63.0^\circ$  elevation, they were  $1.0679 \times 10^{13}$  and  $1.1825 \times 10^{13}$  electrons/cm<sup>2</sup>, respectively.

In deriving the errors defined by Equation (4-1) and shown in Figure 4-11, the mean value of  $N_t'$  ( $\overline{N_t'} = 1.0367 \times 10^{13}$  electrons/cm<sup>2</sup>) and  $N_r'$  ( $\overline{N_r'} = 1.2882 \times 10^{13}$  electrons/cm<sup>2</sup>) were used. The interesting disclosure of Figure 4-11 is the wide separation in the heights, 252 km and 613 km, at which  $\overline{M}$  and  $\overline{H \cos \theta}$ , respectively, are evaluated to obtain zero error. The slopes of the error curves of the vertical and slant electron content are approximately 6.0 and 7.1 km/1%, respectively.

In order to facilitate the analysis of the polarization rotation rate method, the ionosphere is assumed to be horizontally stratified. Equation (2-11) which expresses  $N_t$  in terms of the time rate of change of the polarization angle and the geometric magnetic factor can also be employed for the calculation of  $N_r$  by simply substituting  $\overline{H \cos \theta}$  for  $\overline{M}$ .

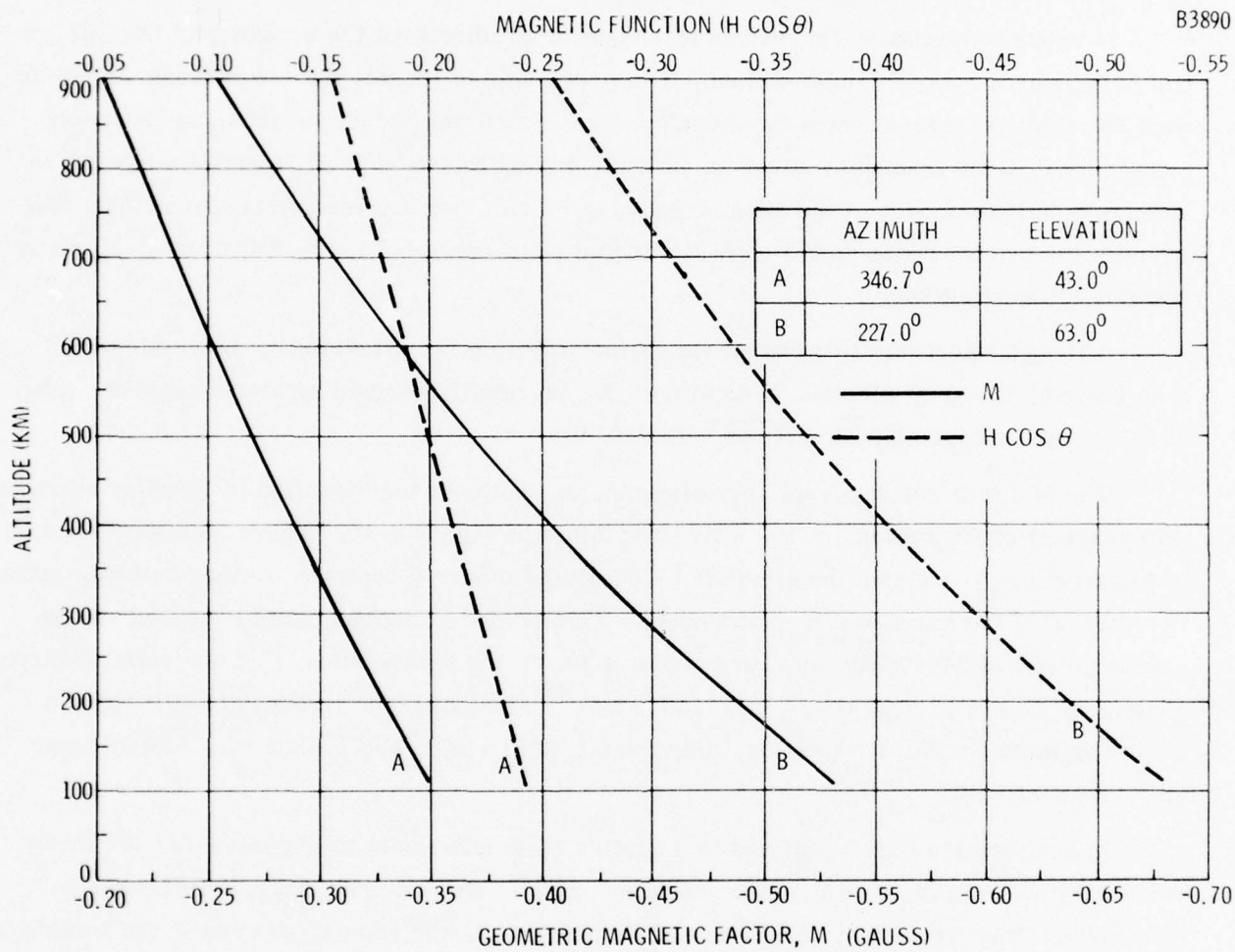


Figure 4-10. The Parameters M and H cos θ in the Directions of Faraday Rotation Difference of  $\pi/2$  Radians at 150 MHz

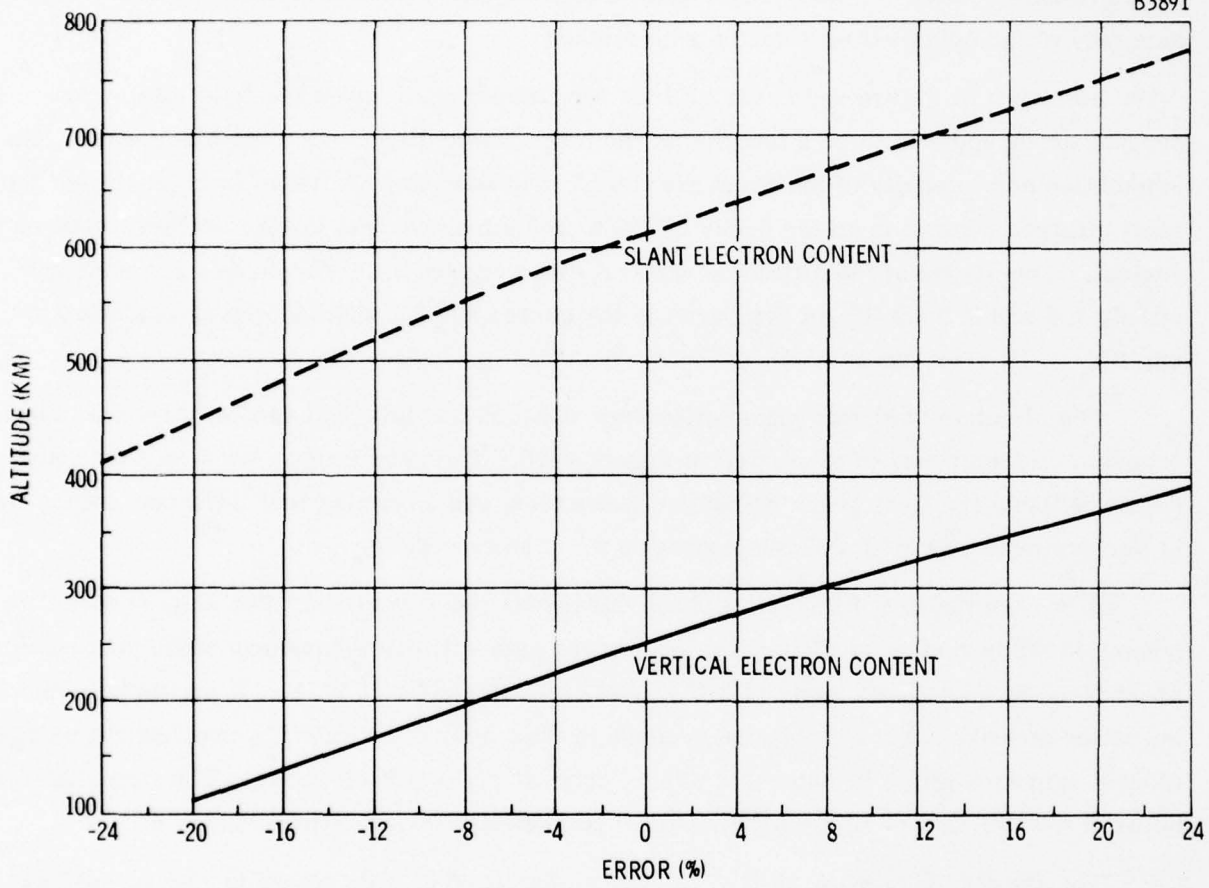


Figure 4-11. Error in Determining the Vertical and Slant Electron Content at 150 MHz by the Differential Polarization Rotation Angle Method

The geometric magnetic factor,  $M$ , and the magnetic function,  $H \cos \theta$ , shown in Figures 4-12 and 4-13, respectively, illustrate the spatial variation of the parameters at constant altitudes in the direction of the satellite trajectory.

The time derivative of  $M$  and  $H \cos \theta$  plotted in Figure 4-14 and the magnitude of the terms listed in Table 4-1 were used, in conjunction with Equation (2-11) to estimate the accuracy of the polarization rotation rate method.

As shown in Figure 4-15, the altitude for computing  $\dot{M}$  and  $\dot{H \cos \theta}$  to attain zero percent error appears to be a function of the propagation direction, or in other words, the orientation and intensity of the magnetic field. It is seen that the mean field height for the slant electron content is on the order of 300 to 400 km above that for the vertical electron content. The slopes of the altitude - vertical electron content error curves are approximately 1.6 and 6.3 km/1% as compared to the corresponding slant-slopes of 4.0 and 8.0 km/1%.

The simulated relative phase difference between the 150- and 400-MHz transmissions received on the ground is presented in Figure 4-16. The calculations are based on Equation (2-23) utilizing the first order refractive index term and assuming that the phase comparison is performed at 150 MHz with the constants  $a = 1$  and  $b = (3/8)$ .

It is seen that the differential phase undergoes two reversals. The first reversal occurs at the beginning of the orbital pass in the high-altitude ionosphere while the second takes place at an azimuth angle of  $287.5^\circ$  and elevation angle of  $71.5^\circ$ . It should be noted that the latter appears approximately 10 seconds in time before the satellite reaches the point of closest approach which is located at  $276.2^\circ$  azimuth and  $71.8^\circ$  elevation. The time difference between the two data points is attributed to the presence of ionization gradients.

The Doppler frequency shift of the two transmitted signals shown in Figure 4-17 are derived on the basis of free space conditions. Because the satellite is in a noncircular orbit, zero Doppler occurs about 3 seconds later in time than the point of closest approach. The zero Doppler-angular coordinates are  $272.9^\circ$  azimuth and  $71.77^\circ$  elevation.

Figure 4-18 which is a plot of the simulated Doppler frequency shift induced by the ionosphere was computed from the second term on the right side of Equation (2-26). As in the case of the differential phase, the higher order terms in the refractive index have been neglected. It is noted that the spatial position of the zero-ionospheric Doppler frequency shift coincides with the second phase reversal point in Figure 4-16.

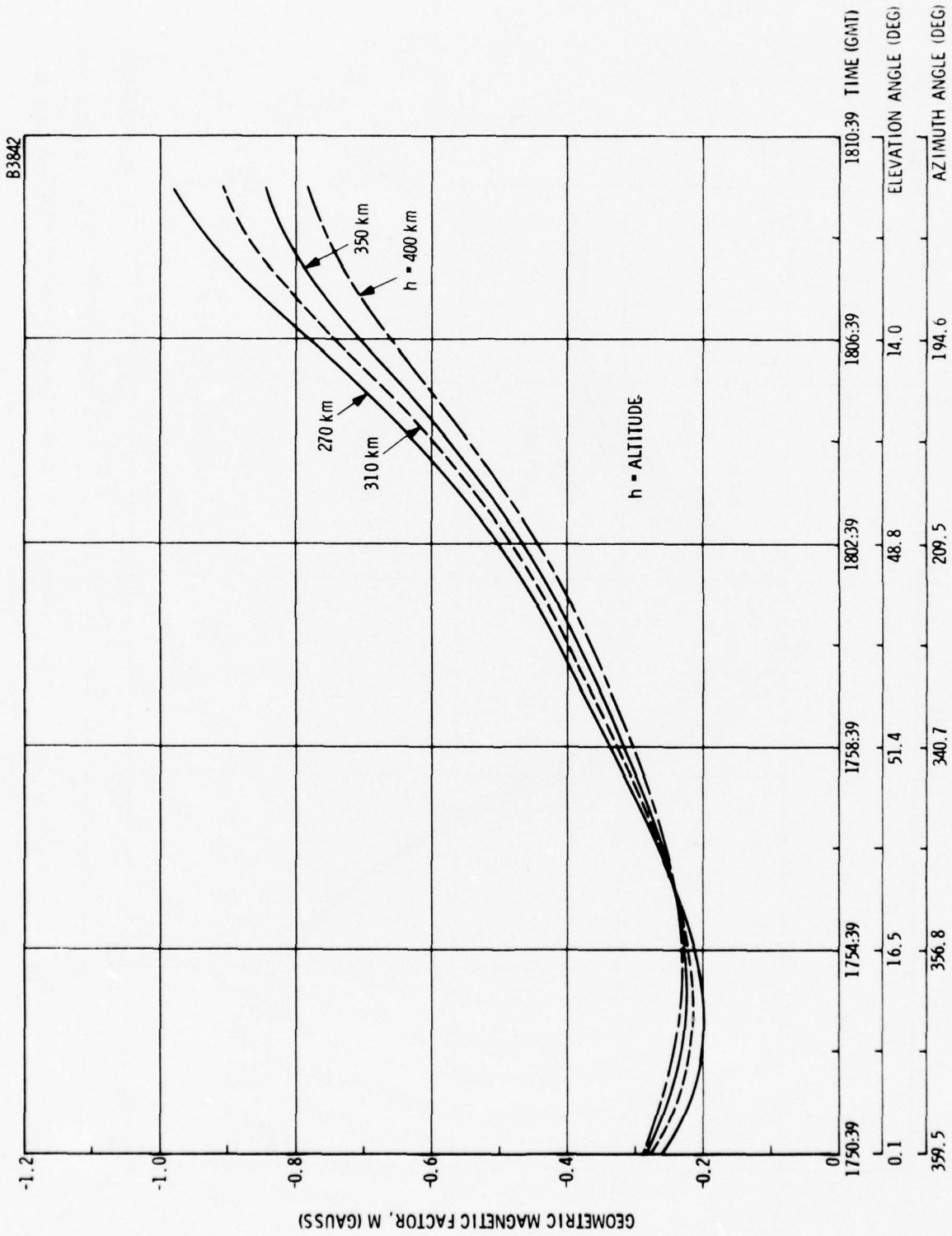


Figure 4-12. Geometric Magnetic Factor, M, As a Function of Altitude Across the Satellite Orbital Pass

B3843

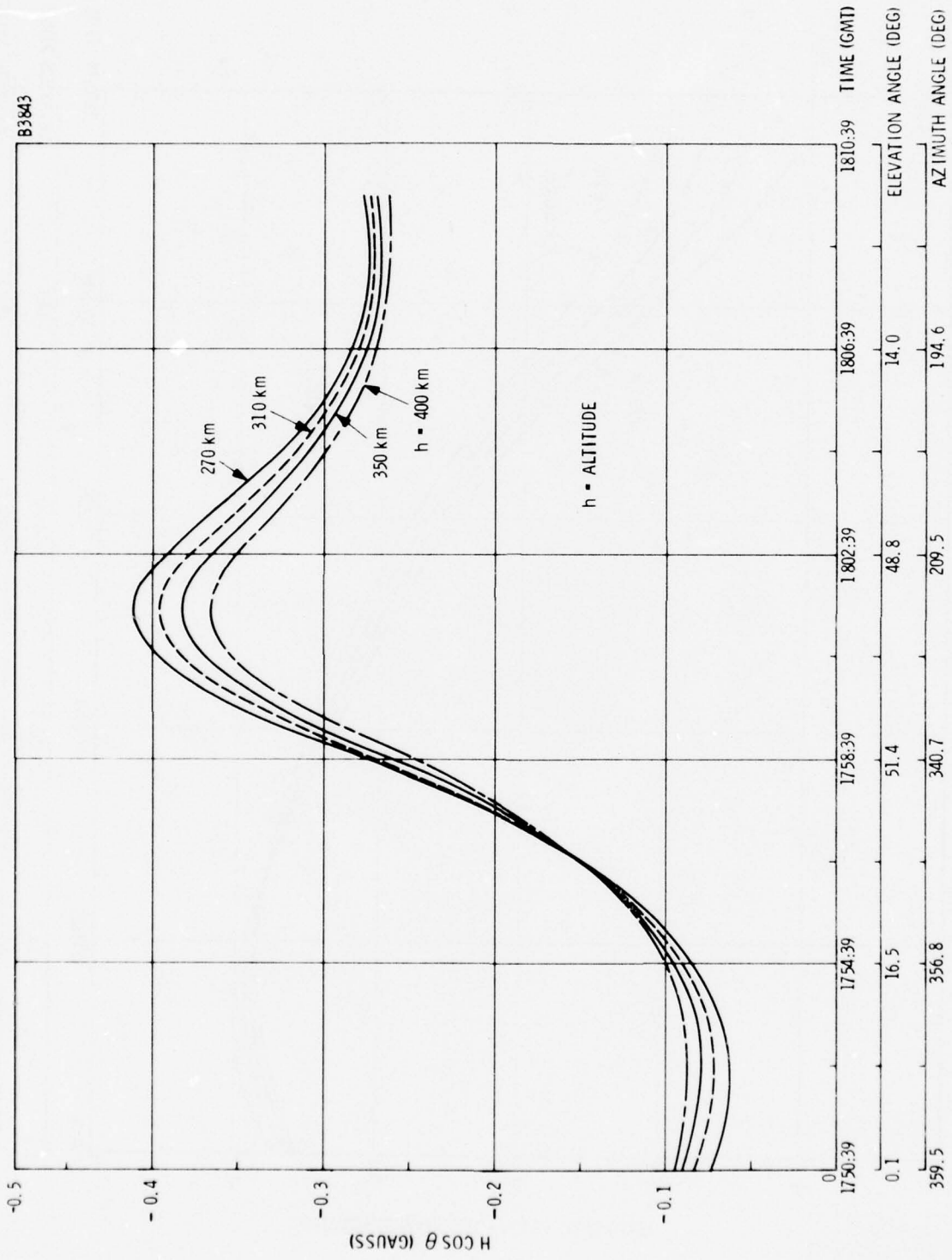


Figure 4-13. Magnetic Function,  $H \cos \theta$ , As a Function of Altitude Across the Satellite Orbital Pass

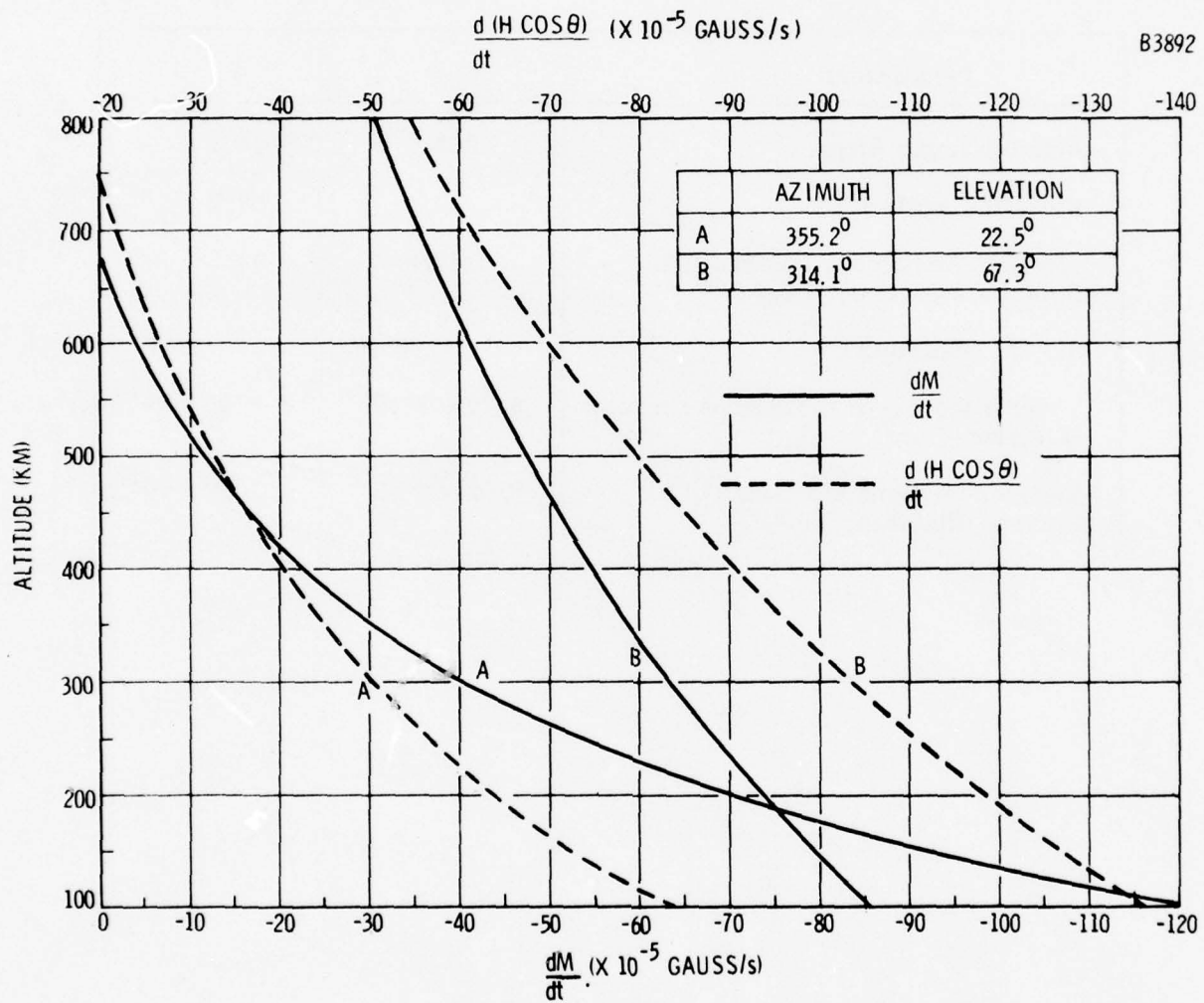


Figure 4-14. Time Derivative of the Parameters M and H cos  $\theta$

TABLE 4-1

PARAMETERS USED IN THE EVALUATION OF THE ACCURACY  
OF THE POLARIZATION ROTATION RATE METHOD

Parameters	A	B
Azimuth Angle (Deg)	355.2	314.1
Elevation Angle (Deg)	22.5	67.3
150 MHz Ambiguous Polarization Rotation Angle, $\Omega$ , (Deg)	43.9	41.7
$d\Omega/dt$ (Rad/sec)	0.00637	0.00715
Theoretical Vertical Electron Content (Electrons/cm <sup>2</sup> )	$9.7042 \times 10^{12}$	$1.0295 \times 10^{13}$
Theoretical Slant Electron Content (Electrons/cm <sup>2</sup> )	$2.0244 \times 10^{13}$	$1.1062 \times 10^{13}$

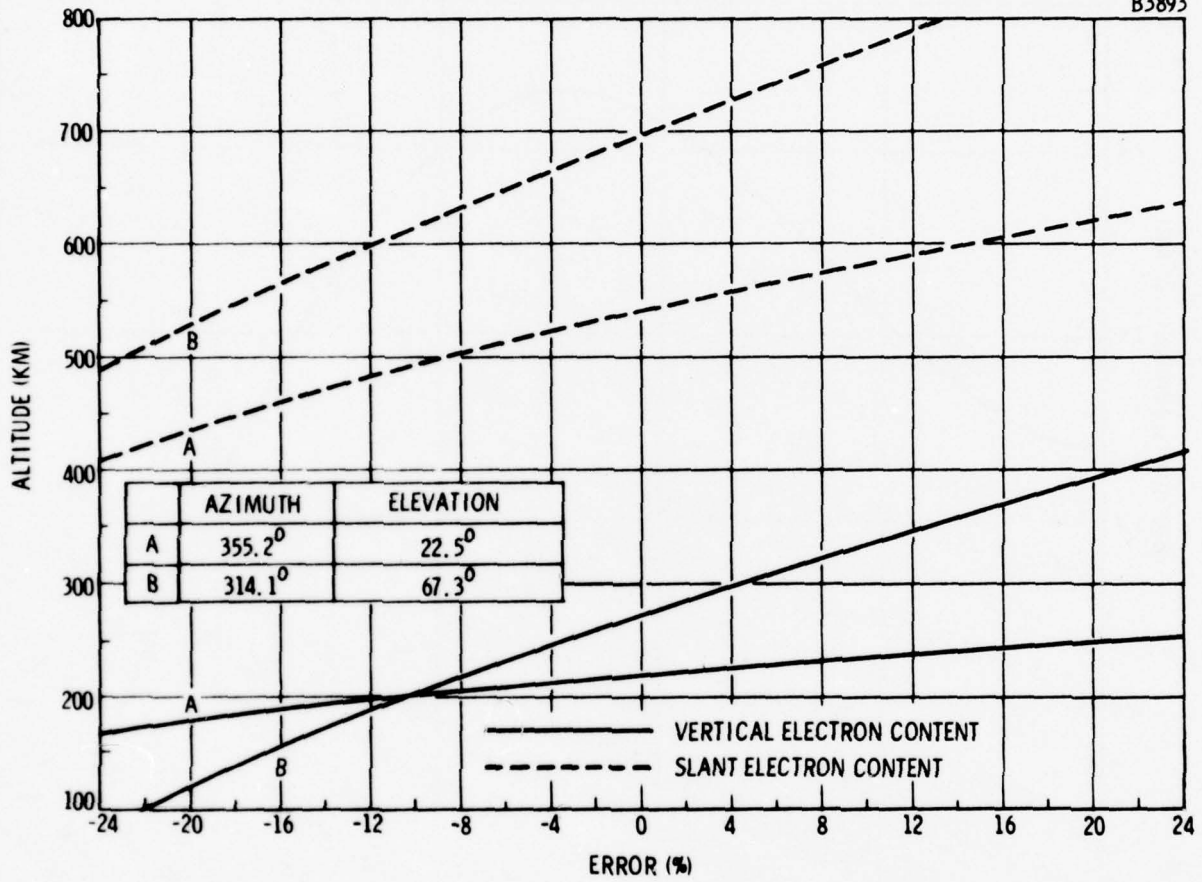


Figure 4-15. Error in Determining the Vertical and Slant Electron Content at 150 MHz by the Polarization Rotation Rate Method

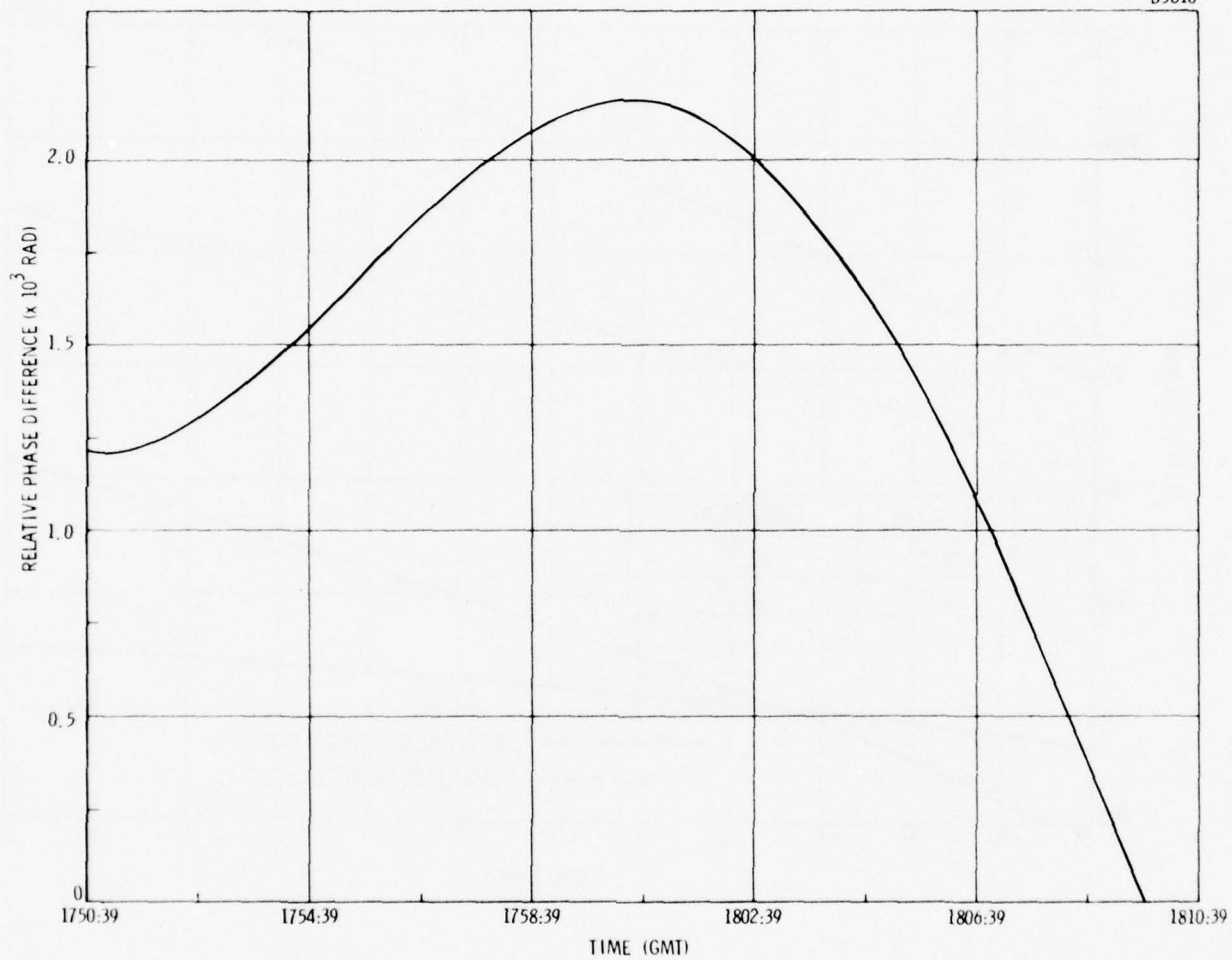


Figure 4-16. Simulated Relative Phase Difference Between 150- and 400-MHz Transmissions from TRANSIT Satellite, Object No. 1970-067A, June 3, 1974

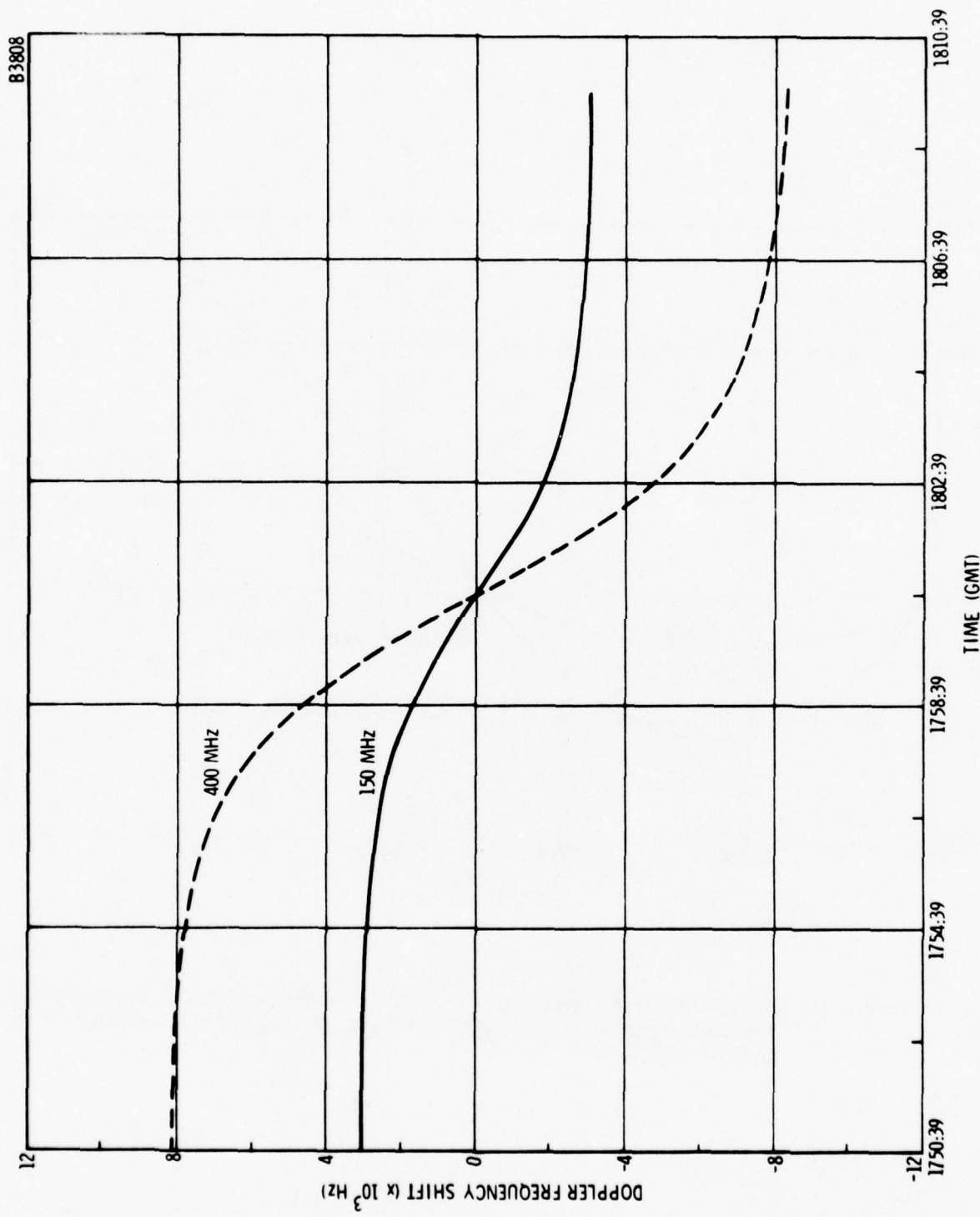


Figure 4-17. Simulated Free Space - Doppler Frequency Shift of 150- and 400-MHz Transmissions From TRANSIT Satellite, Object No. 1970-067A, June 3, 1974

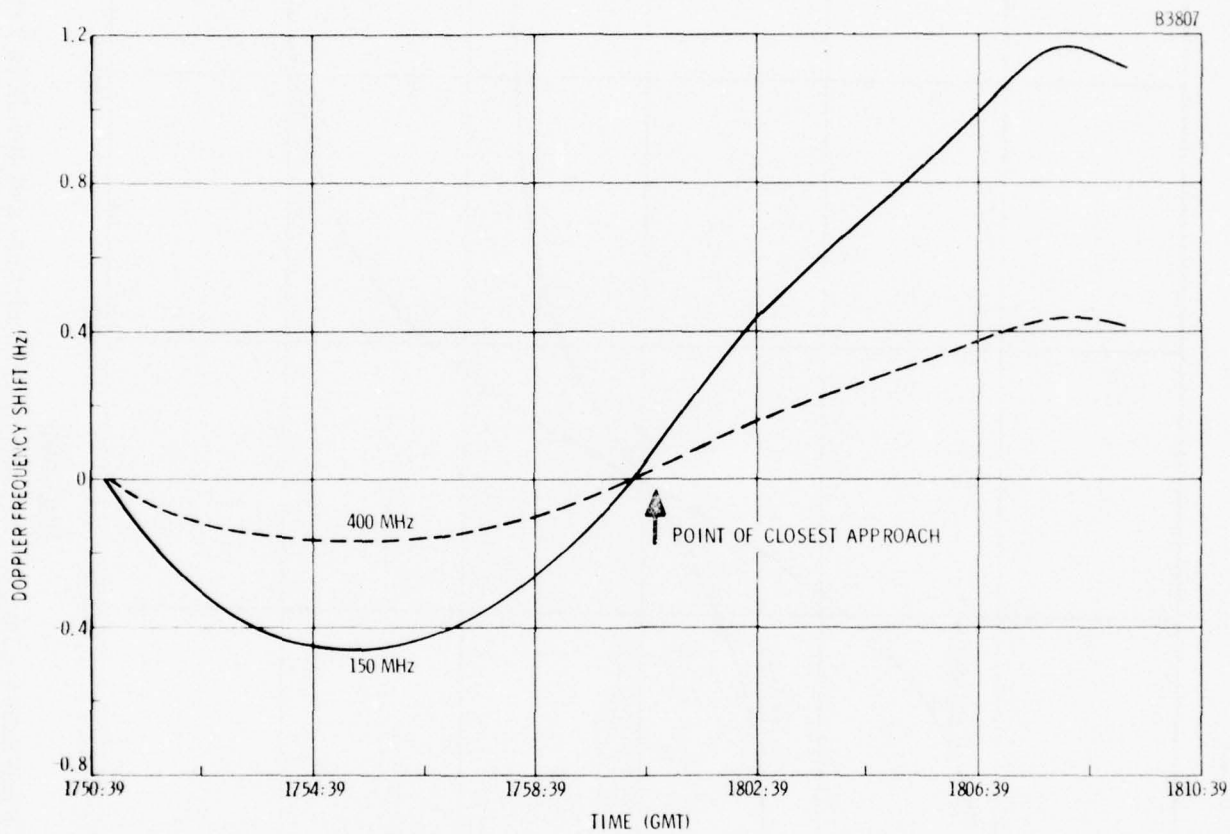


Figure 4-18. Simulated Ionospheric Doppler Frequency Shift of 150- and 400-MHz Transmissions from TRANSIT Satellite, Object No. 1970-067A, June 3, 1974

The conversion of the relative electron content obtained from differential phase measurement into an absolute value can be accomplished by means of the Doppler frequency shift method proposed by Al'pert (1958).

The estimates of the accuracy of this method for four satellite locations near the point of closest approach are contained in Table 4-2, the calculations being based on Equations (2-25), (2-26) and (4-1). It is seen that the error in determining the vertical electron content could vary from -56.5% to +114.4%. It is possible that the accuracy degradation is due to the fact that the satellite is not in a circular orbit.

The Doppler frequency slope method of Arendt et al. (1965), described by Equation (2-27), can also be applied to the electron content calibration.

Table 4-3 lists the values of the parameters at the point of closest approach used in the Doppler slope calculations. It is found that there is a +29.4% error in the estimation of the vertical electron content. It is of interest to note that 100% accuracy would be attained if the satellite is assumed to be at an altitude of 889.5 km.

Vertical incidence ionospheric-sweep frequency soundings in conjunction with the Chapman electron density profile, Equation (2-29), can be employed for the conversion of the differential phase data into an absolute electron content measurement (Evans and Holt, 1973). In applying the Chapman distribution, it is necessary to infer from analytical models the scale height,  $H_s$ , and the height of the F-layer maximum ionization,  $h_m$ . Since the simulated receiver site, i. e., General Electric Radio-Optical Observatory, is approximately 211 km west of the Millstone Hill radar facility, it is valid to assume the models for  $H_s$  and  $h_m$ , Equations (2-31) and (2-32), suggested by Evans and Holt (1973). In addition, it is assumed that the ionosonde can accurately measure the F-layer ordinary wave-critical frequency,  $f_oF2$ , from which, according to Equation (2-30), the maximum electron density of the F-layer,  $N_m$ , can be deduced. It should be noted that, for each one percent error in the  $f_oF2$  determination, a 2% error will be introduced in  $N_m$ .

The results of the analysis of the ionosonde method are summarized in Table 4-4. An error of +11.1% implies, that, for this example, the ionosonde method would give a greater electron content than that stipulated by the Penn State model. This is clearly evident in Figure 4-19 which depicts the true and the ionosonde-predicted electron density profile.

TABLE 4-2  
 ERROR ESTIMATION OF THE DOPPLER FREQUENCY  
 SHIFT METHOD

Azimuth Angle (Deg)	306.6	287.6	255.4	238.7
Elevation Angle (Deg)	69.1	71.5	70.6	67.4
Satellite Altitude (Km)	1153.9	1151.7	1148.5	1146.3
150 MHz Total Doppler Frequency Shift (Hz)	611.43	249.48	-307.39	-667.82
400 MHz Total Doppler Frequency Shift (Hz)	1630.64	665.32	-819.96	-1781.26
Estimated Vertical Electron Content (Electrons/cm <sup>2</sup> )	$7.3443 \times 10^{12}$	$4.5011 \times 10^{12}$	$2.2443 \times 10^{13}$	$1.7280 \times 10^{13}$
Theoretical Vertical Electron Content (Electrons/cm <sup>2</sup> )	$1.0317 \times 10^{13}$	$1.0359 \times 10^{13}$	$1.0468 \times 10^{13}$	$1.0573 \times 10^{13}$
Error (Percent)	-28.8	-56.5	+114.4	+63.4

TABLE 4-3

ERROR ESTIMATION OF THE DOPPLER FREQUENCY  
SLOPE METHOD

Azimuth Angle (Deg)	276.6
Elevation Angle (Deg)	71.8
Satellite Altitude (Km)	1150.7
150 MHz Total Doppler Frequency Slope (Hz/sec)	13.922
400 MHz Total Doppler Frequency Slope (Hz/sec)	37.132
Estimated Vertical Electron Content (Electrons/cm <sup>2</sup> )	$1.3428 \times 10^{13}$
Theoretical Vertical Electron Content (Electrons/cm <sup>2</sup> )	$1.0380 \times 10^{13}$
Error (Percent)	+29.4

TABLE 4-4

## ERROR ESTIMATION OF THE IONOSONDE METHOD

Azimuth Angle (Deg)	276.6
Elevation Angle (Deg)	71.8
Satellite Altitude (Km)	1150.7
Local Time (Hours)	13
Day Number	154
Scale Height (Km)	86.3
Maximum Ionization Height (Km)	245.4
Maximum Electron Density (Electrons/cm <sup>3</sup> )	$3.381 \times 10^5$
Estimated Vertical Electron Content (Electrons cm <sup>2</sup> )	$1.1529 \times 10^{13}$
Theoretical Vertical Electron Content (Electrons/cm <sup>2</sup> )	$1.0380 \times 10^{13}$
Error (Percent)	+11.1

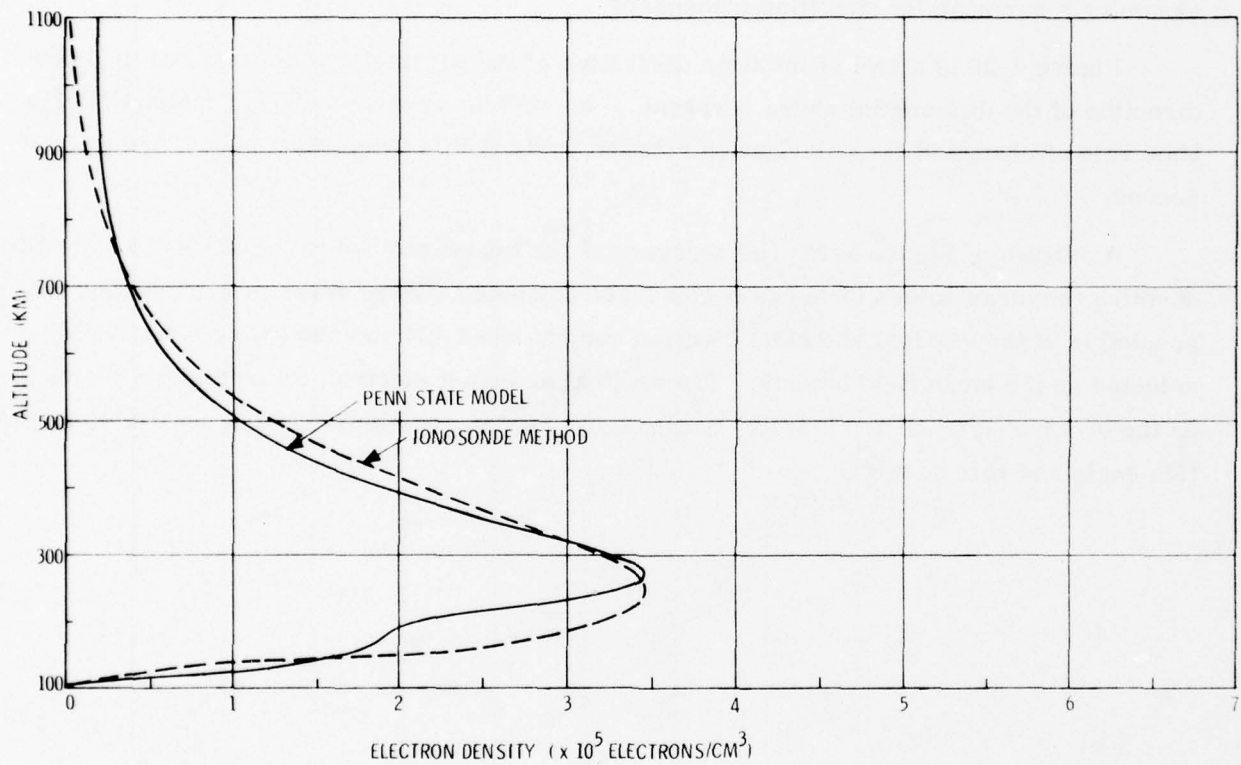


Figure 4-19. Electron Density Profile at Point of Closest Approach of TRANSIT Satellite, Object No. 1970-067A, 1800 Hours GMT, June 3, 1974 at Schenectady, New York as Predicted by the Penn State Ionosphere Model and Ionosonde Method

When Faraday rotation and differential Doppler signals from beacon satellites are simultaneously recorded, the hybrid method proposed by Burgess (1962) can be applied for ionospheric electron content studies. For simplicity, Equation (2-43) is only considered in this analysis. This relationship is applicable for the position on the satellite orbit at which the differential Doppler frequency shift or the time rate of change of the differential phase is zero. It should be noted that, on replacing  $\overline{H \cos \theta}$  with  $\overline{M}$ , Equation (2-43) becomes identical to Equation (2-11) which was derived for the polarization rotation rate method assuming a horizontally stratified ionosphere.

Figure 4-20 is a plot of the time derivative of the parameters  $M$  and  $H \cos \theta$  in the direction of the differential phase reversal, i. e.,  $287.6^\circ$  azimuth and  $71.5^\circ$  azimuth. The time rate of change of the polarization rotation angle at this orientation is  $0.00584$  radian/second.

As shown in Figure 4-21, the accuracy of the hybrid method is dependent on the altitude at which the mean values of  $M$  and  $H \cos \theta$  are computed. Zero error is achieved for the prediction of the vertical and slant electron content when  $454$  and  $602$  km, respectively, are selected as the mean field heights. The vertical and slant electron content error slopes are on the order of  $7.0$  and  $7.7$  km/1%, respectively, which are similar to the polarization rotation angle and rate results.

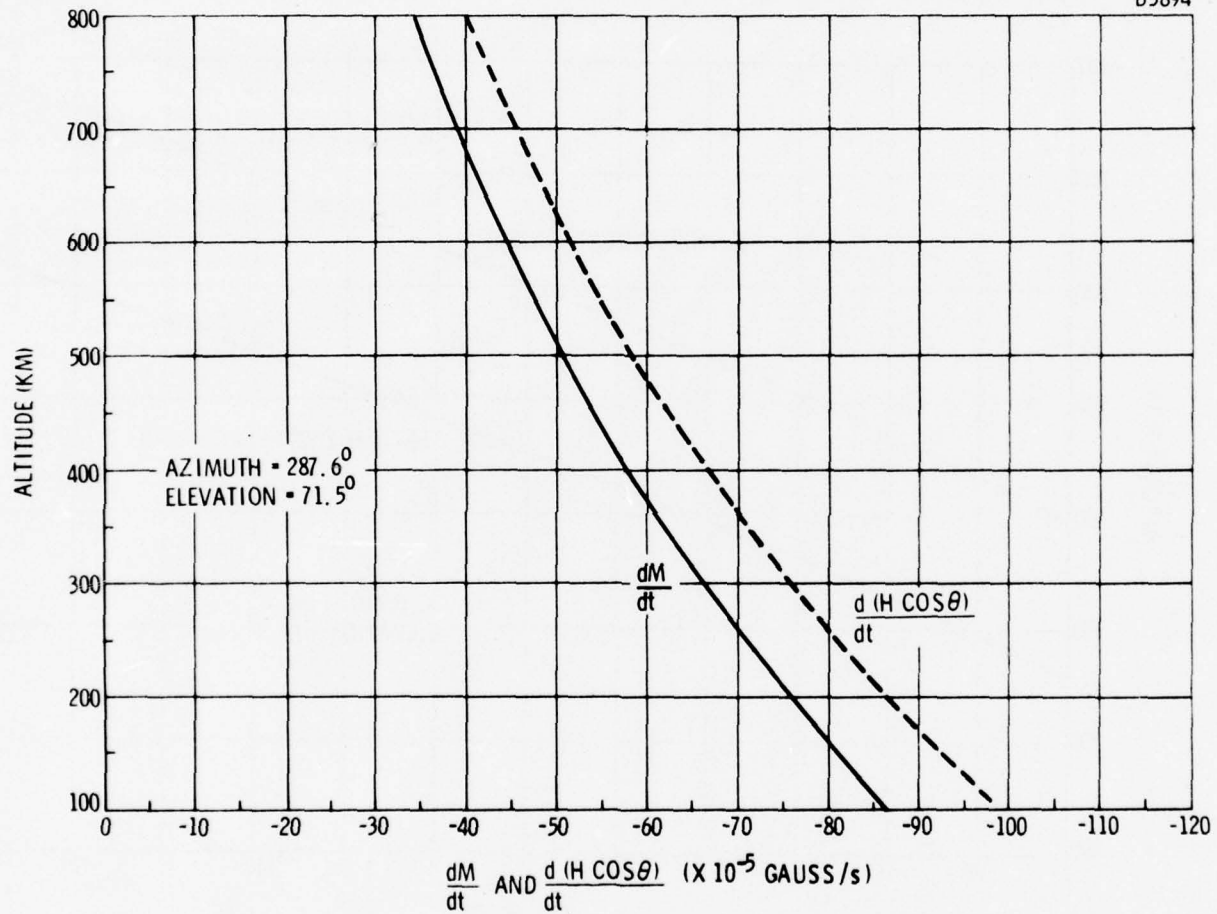


Figure 4-20. Time Derivative of the Parameters  $M$  and  $H \cos \theta$  in the Direction of Differential Phase Reversal

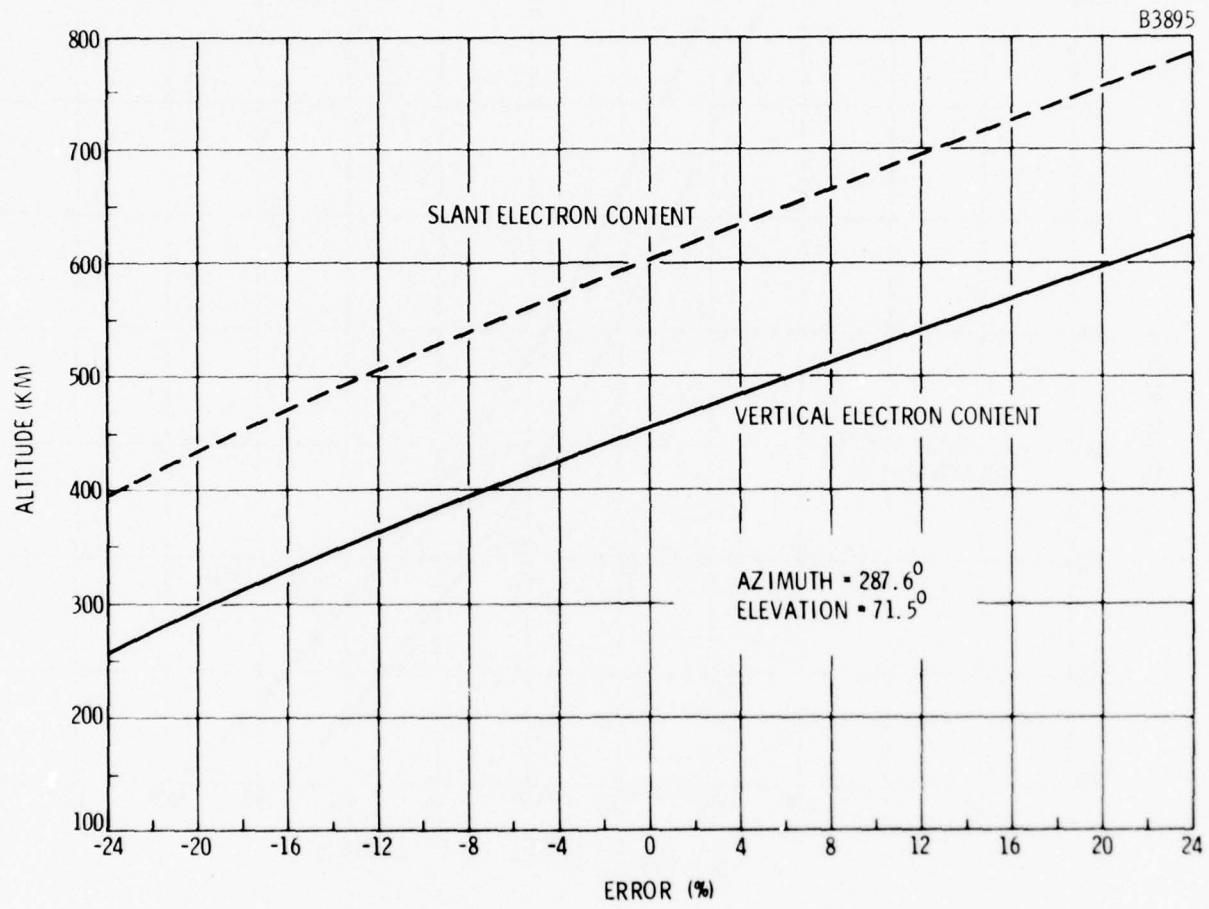


Figure 4-21. Error in Determining the Vertical and Slant Electron Content at 150 MHz by the Faraday-Doppler Hybrid Method

SECTION V  
CONCLUSIONS

It is demonstrated that the concept of computer simulation can be applied for the evaluation of the various analytical techniques for determining the electron content in the ionosphere utilizing beacon satellite transmissions.

The accuracies of the Faraday rotation single frequency, angle and rate methods and the Faraday-Doppler hybrid method are dependent on the altitude at which the mean geometric magnetic factor,  $M$ , and the mean magnetic function,  $\overline{H \cos \theta}$  are evaluated.

The mean field heights for 0% error in the estimation of the vertical and slant electron content are summarized in Table 5-1.

The deviation in the  $\overline{M}$  heights with respect to the F-layer maximum ionization level is found to be within -50 and +184 km.

The mean field heights for  $\overline{H \cos \theta}$  vary from approximately 150 to 425 km above that for  $\overline{M}$  except in the case of the Faraday rotation single frequency method which indicates a height variation ranging from 0 to 28 km.

The errors in predicting the electron content due to inaccuracies in the mean field height are listed in Table 5-2. It appears that a mean field height error has the least effect on the accuracy of the Faraday rotation single frequency method and the greatest on the Faraday rotation rate method.

The electron content prediction accuracy attained by employing the Doppler phenomena is summarized in Table 5-3. Of the three analytical techniques investigated, the ionosonde method seems to be the more accurate.

A more thorough investigation is required to determine the accuracy that can be achieved with the Faraday and Doppler least square method of analysis of beacon satellite signals.

TABLE 5-1  
 ALTITUDE OF  $\overline{M}$  AND  $\overline{H \cos \theta}$  EVALUATION FOR ZERO PERCENT  
 ERROR IN IONOSPHERIC ELECTRON CONTENT ESTIMATION

Analytical Method	Height of F-Layer Peak (km)	Mean Field Height (km)	
		$\overline{M}$	$\overline{H \cos \theta}$
Faraday rotation single frequency	280	354, 360	382, 360
Faraday rotation angle	270	252	613
Faraday rotation rate	270	220, 272	540, 696
Faraday-Doppler hybrid	270	454	602

**TABLE 5-2**  
**ERROR IN IONOSPHERIC ELECTRON CONTENT ESTIMATION DUE TO MEAN**  
**FIELD HEIGHT INACCURACY**

Analytical Method	Altitude-Error Slope (km/1% Error)	
	Vertical Electron Content	Slant Electron Content
Faraday rotation single frequency	14.0, 10.6	14.5, 12.1
Faraday rotation angle	6.0	7.1
Faraday rotation rate	1.6, 6.3	4.0, 8.0
Faraday-Doppler hybrid	7.0	7.7

TABLE 5-3  
ERROR IN IONOSPHERIC ELECTRON CONTENT ESTIMATION UTILIZING  
DISPERSIVE PHASE-DOPPLER TECHNIQUE

Analytical Method	Error (%)
Doppler frequency shift	28.8 - 114.4
Doppler frequency slope	29.4
Ionosonde	11.1

SECTION VI  
REFERENCES

- Al'pert, Y. L., "A Method for Studying the Ionosphere by Means of an Artificial Earth Satellite", *Uspekhi Fizicheskikh Nauk*, Vol. 64, pp 3-14, January-April 1958.
- Arendt, P. R., "Criterion for Application of the Differential Doppler Method", *Nature*, Vol. 212, pp 1342-1343, December 17, 1966.
- Arendt, P. R., A. Papayoanou and H. Soicher, "Determination of the Ionospheric Electron Content Utilizing Satellite Signals", *Proceedings IEEE*, Vol. 53, pp 268-277, March 1965.
- Arendt, P. R. and H. Soicher, "Transionospheric Radio-Ray-Path Rate of Change from Polarization and Frequency Measurements of Satellite VHF Signals", *IEEE Transactions on Antennas and Propagation*, Vol. AP-17, pp 827-828, November 1969.
- Bertin, F. and J. Paper-Lépine, "Latitudinal Variation of Total Electron Content in the Winter at Middle Latitudes", *Radio Science*, Vol. 5, pp 899-906, June 1970.
- Bertin, F., J. Papet-Lépine and E. Vassy, "Geographical Distribution of Total Electron Content Dependence on Geomagnetic Activity", *Radio Science*, Vol. 1, pp 1131-1134, October 1966.
- Bhonsle, R. V., "Diurnal Variation of Large-Scale Ionospheric Irregularities", *Journal of Geophysical Research*, Vol. 71, pp 4571-4577, October 1, 1966.
- Blackband, W. T., "The Determination of Ionospheric Electron Content by Observation of Faraday Fading", *Journal of Geophysical Research*, Vol. 65, pp 1987-1992, July 1960.
- Burgess, B., "Ionospheric Studies Using Satellite Radio Transmissions", in *Electron Density Profiles in the Ionosphere and Exosphere*, NATO Advanced Institute Conference Proceedings, Vol. 2, pp 224-227, Pergamon Press, London, 1962.
- Burgess, B., "Techniques for Analysis of Faraday Fading Data", in *Radio Astronomical and Satellite Studies of the Atmosphere*, pp 313-324, North Holland Publishing Company, Amsterdam, 1963.
- Chapman, S. and J. Bartels, "Geomagnetism", Vols. 1 and 2, Oxford University Press, New York, 1940.

Checacci, P. F., "Ionospheric Measurements by Means of the Early Bird Geostationary Satellite", *Radio Science*, Vol. 1, pp 1154-1158, October 1966.

Crooker, N. U., "An Improvement in the Closely-Spaced Frequencies Method of Deducing Ionospheric Electron Content from Faraday Rotation Measurements", *Journal of Atmospheric and Terrestrial Physics*, Vol. 32, pp 179-185, 1970.

de Mendonça, F., "Ionospheric Electron Content and Variations Measured by Doppler Shifts in Satellite Transmissions", *Journal of Geophysical Research*, Vol. 67, pp 2315-2337, June 1962.

de Mendonça, F., and O.K. Garriott, "Ionospheric Electron Content Calculated by a Hybrid Faraday-Doppler Technique", *Journal of Atmospheric and Terrestrial Physics*, Vol. 24, pp 317-321, 1962.

Evans, J. V. and J.M. Holt, "The Combined Use of Satellite Differential Doppler and Ground-Based Measurements for Ionospheric Studies", *IEEE Transactions on Antennas and Propagation*, Vol. AP-21, pp 685-692, September 1973.

Garriott, O.K. and F. de Mendonça, "A Comparison of Methods Used for Obtaining Electron Content from Satellite Observations", *Journal of Geophysical Research*, Vol. 68, pp 4917-4927, September 1, 1963.

Golton, E., "A Method for the Analysis of Combined Faraday and Differential Doppler Recordings in the Presence of Horizontal Gradients and Vertical Satellite Motion", *Journal of Atmospheric and Terrestrial Physics*, Vol. 24, pp 554-558, 1962.

Golton, E. and G.O. Walker, "Observations of Ionospheric Electron Content Across the Equatorial Anomaly at Sunspot Minimum", *Journal of Atmospheric and Terrestrial Physics*, Vol. 33, pp 1-11, 1971.

IAGA Commission 2 Working Group 4, Analysis of the Geomagnetic Field, "International Geomagnetic Reference Field 1965.0", *Journal of Geophysical Research*, Vol. 74, pp 4407-4408, August 15, 1969.

Kersley, L. and G.N. Taylor, "Comparison of Total Electron Contents from Beacon Satellite Faraday Rotation Measurements and Simultaneous Incoherent Scatter Profiles", *Journal of Atmospheric and Terrestrial Physics*, Vol. 36, pp 93-102, 1974.

Klobuchar, J.H., J. Aarons, and H.H. Hosseinieh, "Midlatitude Nighttime Total Electron Content Behavior During Magnetically Disturbed Periods", *Journal of Geophysical Research, Space Physics*, Vol. 73, pp 7530-7534, December 1, 1968.

Klobuchar, J.A. and R.S. Allen, "A First-Order Prediction Model of Total-Electron-Content Group Path Delay for a Midlatitude Ionosphere", *Air Force Cambridge Research Laboratories, Air Force Surveys in Geophysics No. 222, AFCRL-70-0403*, July 1970.

Klobuchar, J.A. and H.E. Whitney, "Middle-Latitude Ionospheric Total Electron Content: Summer 1965", *Radio Science*, Vol. 1, pp 1149-1154, October 1966.

Lawrence, R.S., D.J. Posakony, O.K. Garriott and S.C. Hall, "The Total Electron Content of the Ionosphere at Middle Latitudes Near the Peak of the Solar Cycle", *Journal Geophysical Research*, Vol. 68, pp 1889-1898, April 1, 1963.

Liszka, L., "Local Electron Densities Deduced from the Faraday Fading of Satellite Transmissions Using Measurements During Two Consecutive Transits", *Planetary Space Science*, Vol. 5, pp 213-219, 1961.

Liszka, L., "Latitudinal and Diurnal Variations of the Ionospheric Electron Content Near the Auroral Zone in Winter", *Radio Science*, Vol. 1, pp 1135-1137, October 1966.

Lyon, G.F., "Satellite Transmission Measurements of Ionospheric Electron Content at a Time of Low Solar Activity", *Canadian Journal of Physics*, Vol. 43, pp 1059-1067, 1965.

Lyon, G.F., "Mid to High Latitude Ionospheric Electron Content", *Journal of Atmospheric and Terrestrial Physics*, Vol. 32, pp 1737-1745, 1970.

Mendillo, M., M.D. Papagiannis and J.A. Klobuchar, "Ionospheric Storms at Midlatitudes", *Radio Science*, Vol. 5, pp 895-898, June 1970.

Merrill, R.G. and R.S. Lawrence, "Ionospheric Electron Content at Midlatitudes Near the Minimum of the Solar Cycle", *Journal of Geophysical Research*, Vol. 74, pp 4661-4665, September 1, 1969.

Millman, G.H., "The Geometry of Radar-Auroral Reflections", *General Electric Technical Information Series Report No. R58EMH3*, March 1958.

Millman, G.H., "The Geometry of the Earth's Magnetic Field at Ionospheric Heights", *Journal of Geophysical Research*, Vol. 64, pp 717-726, July 1959.

Millman, G.H., "Radar-Lunar Measurements of the Electron Content of the Ionosphere", *Journal of Geophysical Research*, Vol. 69, pp 429-440, February 1, 1964.

Millman, G.H., "A Survey of Tropospheric, Ionospheric and Extraterrestrial Effects on Radio Propagation between the Earth and Space Vehicles", in Propagation Factors in Space Communications, AGARD Conference Proceedings No. 3, Technivision, Maidenhead, England, 1967; General Electric Technical Information Series Report No. R66EMH1, January 1966.

Millman, G.H., and R.E. Anderson, "Ionospheric Phase Fluctuations of Satellite Transmissions", Journal of Geophysical Research, Space Physics, Vol. 73, pp 4434-4438, July 1, 1968.

Millman, G.H. and F. Rose, "A Study of Ionospheric and Lunar Characteristics by Radar Techniques", General Electric Technical Information Series Report No. R61EMH40, August 1961.

Münther, C., "Measurement of the Total Electron Content with the Differential Faraday Effect Using the Satellite Explorer 22", Radio Science, Vol. 1, pp 1141-1145, October 1966.

Nisbet, J.S., "On the Construction and Use of the Penn State MK I Ionospheric Model", Pennsylvania State University, Ionosphere Research Laboratory Scientific Report No. 355, May 1970.

Rao, N.N., "Ionospheric Electron Content and Irregularities Deduced from BE-C Satellite Transmissions", Journal of Geophysical Research, Vol. 72, pp 2929-2942, June 1, 1967.

Ratcliffe, J.A., "The Magneto-Ionic Theory and Its Application to the Ionosphere", Cambridge University Press, New York, 1959.

Roger, R.S., "Measurements of the Equivalent Slab Thickness of the Daytime Ionosphere", Journal of Atmospheric and Terrestrial Physics, Vol. 26, pp 475-497, 1964.

Ross, W.J., "The Determination of Ionospheric Electron Content from Satellite Doppler Measurements 1. Method of Analysis", Journal of Geophysical Research, Vol. 65, pp 2601-2606, September 1960a.

Ross, W.J., "The Determination of Ionospheric Electron Content from Satellite Doppler Measurements 2. Experimental Results", Journal of Geophysical Research, Vol. 65, pp 2607-2615, September 1960b.

Ross, W.J., "Second-Order Effects in High-Frequency Transionospheric Propagation", Journal of Geophysical Research, Vol. 70, pp 597-612, February 1, 1970.

Shmelovsky, K. Kh., P. Klinker and R. Knut, "Electron Concentration in the Upper Ionosphere from Observation of the Third Soviet Satellite", *Geomagnetism and Aeronomy*, Vol. III, pp 25-36, 1963.

Smith, D.H., "Removal of the  $n\pi$  Ambiguity in Observations of Total Electron Content", *Journal of Atmospheric and Terrestrial Physics*, Vol. 33, pp 1161-1168, 1971.

Titheridge, J.E., "On the Ambiguity in Faraday Rotation Measurements of the Electron Content of the Ionosphere", *Journal of Atmospheric and Terrestrial Physics*, Vol. 33, pp 1115-1117, 1971.

Titheridge, J.E. "Determination of Ionospheric Electron Content from the Faraday Rotation of Geostationary Satellite Signals," *Planetary Space Science*, Vol. 20, pp 353-369, March 1972.

Tucker, H. J. and B. M. Fannin, "Analysis of Ionospheric Contributions to the Doppler Shift of CW Signals from Artificial Earth Satellites", *Journal of Geophysical Research, Space Physics*, Vol. 73, pp 4325-4334, July 1, 1968.

Wright, J. W., "A Model of the F Region above  $h_{\max} F2$ ", *Journal of Geophysical Research*, Vol. 65, pp 185-191, January 1960.

Yeh, K. C., "Second-Order Faraday Rotation Formulas", *Journal of Geophysical Research*, Vol. 65, pp 2548-2550, August 1960.

Yeh, K. C., private communication, 1974.

Yeh, K. C. and G. W. Swenson, "Ionospheric Electron Content and Its Variations Deduced from Satellite Observations", *Journal of Geophysical Research*, Vol. 66, pp 1061-1067, April 1961.

Yuen, P. C. and T. H. Roelofs, "Diurnal Variation of the Ionospheric Total Electron Content", *Journal of Geophysical Research*, Vol. 71, pp 849-854, February 1, 1966.

## APPENDIX A

### FARADAY POLARIZATION ROTATION EFFECT

When a linearly-polarized electromagnetic wave enters the ionosphere, the wave separates into two independent components both, in the general case, elliptically polarized with opposite senses of rotation. For frequencies in the VHF range and above, the two components, i.e., the ordinary and extraordinary waves, are circularly polarized.

As the ionosphere is traversed, the two waves progress with different velocities of propagation which result in the phase relationship between them to be continuously changing. On leaving the ionosphere, the circularly polarized components recombine to form a linearly polarized wave which is rotated with respect to the original linear wave.

The differential phase shift that each of the components undergoes in an element of path length,  $dr$ , is given by

$$d\phi_o = \frac{2\pi}{\lambda_o} dr \quad (\text{A-1})$$

and

$$d\phi_e = \frac{2\pi}{\lambda_e} dr \quad (\text{A-2})$$

where the subscripts,  $o$  and  $e$ , refer to the ordinary and extraordinary wave, respectively, and  $\lambda_o$  and  $\lambda_e$  are the wavelengths associated with the phase velocity,  $V_{po}$  and  $V_{pe}$ , of the waves.

By definition

$$\lambda_{o,e} = \frac{V_{po,e}}{f} \quad (\text{A-3})$$

and

$$V_{po,e} = \frac{c}{n_{o,e}} \quad (\text{A-4})$$

where  $c$  is the free space velocity,  $f$  is the transmission frequency, and  $n_{o,e}$  are the refractive indices of the medium.

Since the angular rotation of the plane of polarization of the wave,  $d\Omega$ , as it travels the distance,  $dr$ , is given by

$$d\Omega = \frac{1}{2} (d\phi_o - d\phi_e) \quad (\text{A-5})$$

it follows from Equations (A-1) through (A-4) that

$$d\Omega = \frac{\omega}{2c} \Delta n dr \quad (\text{A-6})$$

where  $\omega = 2\pi f$  and  $\Delta n = n_o - n_e$ .

This relationship defines the angular rotation of a linearly polarized for a one-way propagation path. When a two-way transmission path is considered, an additional factor of 2 is introduced.

Thus, the total polarization shift (in radians) for a one-way propagation path in terms of a vertical height variable,  $dh$ , becomes

$$\Omega = \frac{\omega}{2c} \int_{h_1}^{h_2} \Delta n f(h) dh \quad (\text{A-7})$$

where  $h_1$  and  $h_2$  are the height limits of the path.

The function,  $f(h)$ , which is the secant of the angle between the ray path and the zenith, is given by

$$f(h) = \frac{r_o + h}{\left[ (r_o + h)^2 - (r_o \cos E)^2 \right]^{\frac{1}{2}}} \quad (\text{A-8})$$

where  $r_o$  is the radius of the earth and  $E$  is the elevation angle of the antenna beam.

According to Appendix C, the difference in the refractive indices between the ordinary and the extraordinary waves, for quasi-longitudinal propagation, is

$$\Delta n = \frac{\omega^2 N \omega H}{\omega^3} \cos \theta + \frac{\omega^2 N \omega H^3}{\omega^5} \cos^3 \theta + \frac{1}{2} \frac{\omega^4 N \omega H}{\omega^5} \cos \theta + \dots \quad (\text{A-9})$$

where  $\omega_H$  is the angular gyromagnetic frequency of the electron about the earth's magnetic field,  $\omega_N$  is the angular plasma frequency of the ionosphere and  $\theta$  is the propagation angle.

It follows that the one-way polarization shift can therefore be written as

$$\begin{aligned} \Omega = & \frac{1}{c \omega^2} \int_{h_1}^{h_2} \omega_N^2 \omega_H \cos \theta f(h) dh \\ & + \frac{1}{2c \omega^4} \int_{h_1}^{h_2} \omega_N^2 \omega_H^3 \cos^3 \theta f(h) dh \\ & + \frac{1}{4c \omega^4} \int_{h_1}^{h_2} \omega_N^4 \omega_H \cos \theta f(h) dh + \dots \end{aligned} \quad (A-10)$$

On substituting the parameters defining  $\omega_N^2$  and  $\omega_H$  from Appendix C, this relationship is modified to

$$\begin{aligned} \Omega = & \frac{e^3}{2\pi m_e^2 c^2 f^2} \int_{h_1}^{h_2} N_e H \cos \theta f(h) dh \\ & + \frac{e^5}{8\pi^3 m_e^4 c^4 f^4} \int_{h_1}^{h_2} N_e H^3 \cos^3 \theta f(h) dh \\ & + \frac{e^5}{4\pi^2 m_e^3 c^2 f^4} \int_{h_1}^{h_2} N_e^2 H \cos \theta f(h) dh + \dots \end{aligned} \quad (A-11)$$

where  $e$  is the electron charge,  $m_e$  is the electron mass, and  $N_e$  is the electron density and  $H$  is the magnetic field intensity.

When utilizing the numerical values of the constants as given in Appendix C, the polarization rotation in cgs units is simplified to

$$\begin{aligned}
 \Omega = & \frac{2.3617 \times 10^4}{f^2} \int_{h_1}^{h_2} N_e H \cos \theta f(h) dh \\
 & + \frac{1.8493 \times 10^{17}}{f^4} \int_{h_1}^{h_2} N_e H^3 \cos^3 \theta f(h) dh \\
 & + \frac{9.5166 \times 10^{11}}{f^4} \int_{h_1}^{h_2} N_e^2 H \cos \theta f(h) dh + \dots
 \end{aligned} \tag{A-12}$$

It should be noted that the first term in Equation (A-12) is generally used for polarization rotation calculations. The effect of neglecting the higher order terms in the complete expression for  $\Omega$  has been investigated by Yeh (1960) and Ross (1965).

It is seen in Equations (A-11) and (A-12) that the magnitude of the polarization rotation angle is basically a function of the integrated electron density, the magnetic field intensity,  $H$ , and the propagation angle,  $\theta$ .

It can be shown (Millman, 1959) that the angle  $\theta$  is given by

$$\theta = \cos^{-1} [-\cos \epsilon \sin I - \sin \epsilon \cos I \cos (\gamma - D)] \tag{A-13}$$

where  $I$  and  $D$  are the magnetic inclination and declination angles, respectively. These parameters specify the direction of the total magnetic intensity vector in space.

The angle,  $\epsilon$ , which is the angle between the ray path and the zenith at the point of magnetic field intersection, is defined by

$$\epsilon = \sin^{-1} \left[ \frac{r_o}{r_o + h} \cos E \right] \tag{A-14}$$

It is noted that  $\epsilon$  is related to the function,  $f(h)$ , Equation (A-8), by

$$\epsilon = \sec^{-1} f(h) \quad (\text{A-15})$$

The angle  $\gamma$  which is the geographic azimuth bearing of the radar location as measured at the subionospheric point, i.e., the location on the earth's surface directly beneath the magnetic field intersection point, can be derived from the relationship (Millman, 1958).

$$\gamma = \tan^{-1} \left[ \frac{\sin (\lambda_R - \lambda_P) \cos \phi_R}{\sin \phi_R \cos \phi_P - \cos \phi_R \sin \phi_P \cos (\lambda_R - \lambda_P)} \right] \quad (\text{A-16})$$

where  $\phi$  and  $\lambda$  are the geographic latitude and east longitude, respectively. The subscripts, R and P, refer to the radar site and reflection point, respectively.

The parameters I and D can be deduced from a spherical harmonic model of the earth's magnetic field. The spherical harmonic representation assumes that the earth's main field, i.e., the magnetic field that excludes such phenomena as magnetic disturbances and diurnal variations, can be described by a regular or dipole field and an irregular field.

According to Chapman and Bartels (1940), the magnetic inclination and declination angles for the spherical harmonic model are defined by

$$I = \tan^{-1} \left[ \frac{Z}{(X^2 + Y^2)^{\frac{1}{2}}} \right] \quad (\text{A-17})$$

$$D = \tan^{-1} \left[ \frac{Y}{X} \right] \quad (\text{A-18})$$

where X, Y, and Z are the northward horizontal, the eastward horizontal, and the downward vertical component, respectively, of the total magnetic field intensity, H, which is given by

$$H = \left[ X^2 + Y^2 + Z^2 \right]^{\frac{1}{2}} \quad (\text{A-19})$$

The components, X, Y and Z, are related to the magnetic potential, V, by the functions

$$X = \frac{1}{r} \frac{\partial V}{\partial \phi'} \quad (\text{A-20})$$

$$Y = - \frac{1}{r \sin \phi'} \frac{\partial V}{\partial \lambda} \quad (\text{A-21})$$

$$Z = \frac{\partial V}{\partial r} \quad (\text{A-22})$$

$$V = \sum_{n=0}^{\infty} \sum_{m=0}^n \frac{r_0^{n+1}}{r^{n+1}} \left[ g_{nm} \cos(m\lambda) + h_{nm} \sin(m\lambda) \right] P_n^m(\cos \phi') \quad (\text{A-23})$$

where  $r$  is the distance from the center of the earth,  $\phi'$  is the geographic colatitude,  $P_n^m(\cos \phi')$  are the associated Legendre functions of degree  $n$  and order  $m$ , and  $g_{nm}$  and  $h_{nm}$  are the coefficients of the spherical harmonic expansion. It is noted that the first-degree harmonic terms in Equation (A-23), i.e., terms with  $n = 1$  and  $m = 0$ , reduce to that of a dipole potential.

## APPENDIX B

### DIFFERENTIAL PHASE AND DOPPLER FREQUENCY SHIFT

The phase of an RF signal received on the ground from a transmitter in a satellite can be represented by

$$\phi = \omega t - \frac{2\pi}{\lambda} P_{ti} \quad (B-1)$$

where  $\phi$  is the phase in radians,  $\omega$  is the transmitted angular frequency,  $t$  is the time, and  $\lambda$  is the transmitted wavelength. The parameter  $P_{ti}$  is the phase path length which is given by

$$P_{ti} = \int_0^R (n_t + n_i) dr \quad (B-2)$$

where  $n_t$  and  $n_i$  are the indices of refraction of the troposphere and ionosphere, respectively, and  $dr$  is the element of path length.

For a satellite which transmits two harmonically related coherent frequencies,  $f_1$  and  $f_2$ , the phase of the received signals can be written as

$$\phi_1 = \omega_1 t - \frac{2\pi}{\lambda_1} \int_0^R n_{t1} dr - \frac{2\pi}{\lambda_1} \int_0^R n_{i1} dr \quad (B-3)$$

$$\phi_2 = \omega_2 t - \frac{2\pi}{\lambda_2} \int_0^R n_{t2} dr - \frac{2\pi}{\lambda_2} \int_0^R n_{i2} dr \quad (B-4)$$

where the subscripts, 1 and 2, refers to the two frequencies.

The nonionospheric terms can be eliminated by deriving the phase difference between the two signals which can be expressed by

$$\Delta\phi = a \phi_1 - b \phi_2 \quad (B-5)$$

where the constants a and b are related to the frequency ratio

$$\frac{f_2}{f_1} = \frac{a}{b} \quad (\text{B-6})$$

Since the index of refraction in the troposphere is independent of frequency for frequencies less than approximately 15 GHz, the phase difference evaluates to

$$\Delta\phi = 2\pi \left[ \frac{b}{\lambda_2} \int_0^R n_{i2} dr - \frac{a}{\lambda_1} \int_0^R n_{i1} dr \right] \quad (\text{B-7})$$

As derived in Appendix C, the ionospheric refractive index is given by

$$n = 1 - \frac{1}{2} \frac{\omega_N^2}{\omega^2} \pm \frac{1}{2} \frac{\omega_N^2 \omega_H}{\omega^3} \cos \theta - \frac{1}{2} \frac{\omega_N^2 \omega_H^2}{\omega^4} \cos^2 \theta - \frac{1}{8} \frac{\omega_N^4}{\omega^4} \pm \frac{1}{2} \frac{\omega_N^2 \omega_H^3}{\omega^5} \cos^3 \theta \pm \frac{1}{4} \frac{\omega_N^4 \omega_H}{\omega^5} \cos \theta + \dots \quad (\text{B-8})$$

where  $\omega_N$  is the plasma frequency,  $\omega_H$  is the gyromagnetic frequency of the electrons and  $\theta$  is the propagation angle. For simplicity, the subscript i is no longer retained. The positive signs of the  $\pm$  terms are associated with the ordinary wave while the negative with the extraordinary wave.

Substituting Equation (B-8) in Equation (B-7), there results

$$\begin{aligned}
 \Delta\phi = 2\pi & \left\{ \left( \frac{b}{\lambda_2} - \frac{a}{\lambda_1} \right) R - \frac{1}{2} \left( \frac{b}{\lambda_2 \omega_2^2} - \frac{a}{\lambda_1 \omega_1^2} \right) \int_0^R \omega_N^2 dr \right. \\
 & \pm \frac{1}{2} \left( \frac{b}{\lambda_2 \omega_2^3} - \frac{a}{\lambda_1 \omega_1^3} \right) \int_0^R \omega_N^2 \omega_H \cos \theta dr \\
 & - \frac{1}{2} \left( \frac{b}{\lambda_2 \omega_2^4} - \frac{a}{\lambda_1 \omega_1^4} \right) \int_0^R \omega_N^2 \omega_H^2 \cos^2 \theta dr \\
 & - \frac{1}{8} \left( \frac{b}{\lambda_2 \omega_2^4} - \frac{a}{\lambda_1 \omega_1^4} \right) \int_0^R \omega_N^4 dr \\
 & \pm \frac{1}{2} \left( \frac{b}{\lambda_2 \omega_2^5} - \frac{a}{\lambda_1 \omega_1^5} \right) \int_0^R \omega_N^2 \omega_H^3 \cos^3 \theta dr \\
 & \left. \pm \frac{1}{4} \left( \frac{b}{\lambda_2 \omega_2^5} - \frac{a}{\lambda_1 \omega_1^5} \right) \int_0^R \omega_N^4 \omega_H \cos \theta dr + \dots \right\} \tag{B-9}
 \end{aligned}$$

When utilizing Equation (B-6), this expression reduces to

$$\begin{aligned}
 \Delta\phi = & -\frac{1}{2c\omega_1} \left( \frac{b^2 - a^2}{a} \right) \int_0^R \omega_N^2 dr \\
 & \pm \frac{1}{2c\omega_1^2} \left( \frac{b^3 - a^3}{a^2} \right) \int_0^R \omega_N^2 \omega_H \cos \theta dr \\
 & - \frac{1}{2c\omega_1^3} \left( \frac{b^4 - a^4}{a^3} \right) \int_0^R \omega_N^2 \omega_H^2 \cos^2 \theta dr \\
 & - \frac{1}{8c\omega_1^3} \left( \frac{b^4 - a^4}{a^3} \right) \int_0^R \omega_N^4 dr \\
 & \pm \frac{1}{2c\omega_1^4} \left( \frac{b^5 - a^5}{a^4} \right) \int_0^R \omega_N^2 \omega_H^3 \cos^3 \theta dr \\
 & \pm \frac{1}{4c\omega_1^4} \left( \frac{b^5 - a^5}{a^4} \right) \int_0^R \omega_N^4 \omega_H \cos \theta dr + \dots
 \end{aligned} \tag{B-10}$$

Further simplification can be attained on substituting in the definitions of  $\omega_N^2$  and  $\omega_H$  given in Appendix C. It follows that

$$\begin{aligned}
 \Delta\phi = & -\frac{e^2}{m_e c f_1} \left( \frac{b^2 - a^2}{a} \right) \int_0^R N_e dr \\
 & \pm \frac{e^3}{2\pi m_e^2 c^2 f_1^2} \left( \frac{b^3 - a^3}{a^2} \right) \int_0^R N_e H \cos \theta dr \\
 & - \frac{e^4}{2\pi m_e^3 c^3 f_1^3} \left( \frac{b^4 - a^4}{a^3} \right) \int_0^R N_e H^2 \cos^2 \theta dr \\
 & - \frac{e^4}{4\pi m_e^2 c f_1^3} \left( \frac{b^4 - a^4}{a^3} \right) \int_0^R N_e^2 dr \\
 & \pm \frac{e^5}{8\pi^3 m_e^4 c^4 f_1^4} \left( \frac{b^5 - a^5}{a^4} \right) \int_0^R N_e H^3 \cos^3 \theta dr \\
 & \pm \frac{e^5}{4\pi^2 m_e^3 c^2 f_1^4} \left( \frac{b^5 - a^5}{a^4} \right) \int_0^R N_e^2 H \cos \theta dr + \dots
 \end{aligned} \tag{B-11}$$

where  $e$  is the electron charge,  $m_e$  is the electron mass,  $N_e$  is the electron density and  $H$  is the magnetic field intensity.

It is of interest to note that except for the constants  $a$  and  $b$ , the 2nd, 5th and last term on the right side of Equation (B-11) are identical to the Faraday rotation terms derived in Equation (A-11) of Appendix A.

When the values of the constants are used, the phase difference reduces to

$$\begin{aligned}
 \Delta\phi = & - \frac{8.4396 \times 10^{-3}}{f_1} \left( \frac{b^2 - a^2}{a} \right) \int_0^R N_e \, dr \\
 & \pm \frac{2.3617 \times 10^4}{f_1^2} \left( \frac{b^3 - a^3}{a^2} \right) \int_0^R N_e H \cos \theta \, dr \\
 & - \frac{4.1524 \times 10^{11}}{f_1^3} \left( \frac{b^4 - a^4}{a^3} \right) \int_0^R N_e H^2 \cos^2 \theta \, dr \\
 & - \frac{1.7004 \times 10^5}{f_1^3} \left( \frac{b^4 - a^4}{a^3} \right) \int_0^R N_e^2 \, dr \\
 & \pm \frac{1.8493 \times 10^{17}}{f_1^4} \left( \frac{b^5 - a^5}{a^4} \right) \int_0^R N_e H^3 \cos^3 \theta \, dr \\
 & \pm \frac{9.5166 \times 10^{11}}{f_1^4} \left( \frac{b^5 - a^5}{a^4} \right) \int_0^R N_e^2 H \cos \theta \, dr + \dots
 \end{aligned} \tag{B-12}$$

It should be noted that the phase difference, Equations (B-10) through (B-12) can also be expressed in terms of the frequency  $f_2$ . For this case, the constant  $a$  in the denominators of all the terms is replaced by the constant  $b$ .

The derivation of the phase difference equations is based on the supposition that the propagation paths of the two frequencies are identical. In other words, the ionospheric effects are assumed to be negligible. This assumption is justified, for the most part, for frequencies in the VHF and UHF range except perhaps for propagation at low elevation angles (Millman, 1965).

The frequency of a radio signal emitted from a space vehicle and received on the earth experiences an apparent shift. The phenomenon often being referred to the Doppler effect occurs because of the relative motion between the transmission source and the stationary receiver terminal.

The nonrelativistic Doppler frequency shift,  $f_d$ , in the ionosphere can be defined by the relationship

$$f_d = -\frac{f}{c} \frac{dP}{dt} = -\frac{f}{c} \frac{d}{dt} \int_0^R n \, dr = -\frac{1}{2\pi} \frac{d\phi}{dt} \quad (\text{B-13})$$

On substituting in the definition of the refractive index, Equation (B-8), there results

$$\begin{aligned} f_d &= -\frac{f}{c} \dot{R} + \frac{e^2}{2\pi m_e c f} \frac{d}{dt} \int_0^R N_e \, dr \\ &+ \frac{e^3}{4\pi^2 m_e^2 c^2 f^2} \frac{d}{dt} \int_0^R N_e H \cos \theta \, dr \\ &+ \frac{e^4}{4\pi^2 m_e^3 c^3 f^3} \frac{d}{dt} \int_0^R N_e H^2 \cos^2 \theta \, dr \\ &+ \frac{e^4}{8\pi^2 m_e^2 c f^3} \frac{d}{dt} \int_0^R N_e^2 \, dr \\ &+ \frac{e^5}{16\pi^4 m_e^4 c^4 f^4} \frac{d}{dt} \int_0^R N_e H^3 \cos^3 \theta \, dr \\ &+ \frac{e^5}{8\pi^3 m_e^3 c^2 f^4} \frac{d}{dt} \int_0^R N_e^2 H \cos \theta \, dr + \dots \end{aligned} \quad (\text{B-14})$$

It can be readily shown that Equation (B-14) simplifies to

$$\begin{aligned}
 f_d = & -\frac{f}{c} \dot{R} + \frac{1.3432 \times 10^{-3}}{f} \frac{d}{dt} \int_0^R N_e dr \\
 & + \frac{3.7588 \times 10^3}{f^2} \frac{d}{dt} \int_0^R N_e H \cos \theta dr \\
 & + \frac{6.6088 \times 10^{10}}{f^3} \frac{d}{dt} \int_0^R N_e H^2 \cos^2 \theta dr \\
 & + \frac{2.7063 \times 10^4}{f^3} \frac{d}{dt} \int_0^R N_e^2 dr \\
 & + \frac{2.9433 \times 10^{16}}{f^4} \frac{d}{dt} \int_0^R N_e H^3 \cos^3 \theta dr \\
 & + \frac{1.5146 \times 10^{11}}{f^4} \frac{d}{dt} \int_0^R N_e^2 H \cos \theta dr
 \end{aligned} \tag{B-15}$$

The first term in Equations (B-14) and (B-15) describes the Doppler frequency shift for an object moving in free space. It is seen that the Doppler shift is a function of the time derivative of the integrated electron density along the propagation path in the ionosphere, the Faraday polarization rotation and the refractive bending terms.

The magnitude of the terms in the Doppler frequency expression has been evaluated by Tucker and Fannin (1968).

## APPENDIX C

### IONOSPHERIC INDEX OF REFRACTION

The index of refraction in the ionosphere in the absence of electron collisions, i.e., absorption, is defined by Ratcliffe (1959)

$$n^2 = 1 - \frac{2X(1-X)}{2(1-X) - Y_T^2 \pm \left[ Y_T^4 + 4Y_L^2(1-X)^2 \right]^{\frac{1}{2}}} \quad (\text{C-1})$$

where

$$X = \left( \frac{\omega_N}{\omega} \right)^2 \quad (\text{C-2})$$

$$Y_T = \frac{\omega_H}{\omega} \sin \theta \quad (\text{C-3})$$

$$Y_L = \frac{\omega_H}{\omega} \cos \theta \quad (\text{C-4})$$

where  $\theta$  is the propagation angle, i.e., the angle between the magnetic field vector and the direction of propagation.

The parameter,  $\omega_H$ , is the angular gyromagnetic frequency of the electron about the earth's magnetic field and is given by

$$\omega_H = \frac{H e}{m_e c} \quad (\text{C-5})$$

where  $H$  is the magnetic field intensity in gauss,  $e$  is the electron charge ( $4.8 \times 10^{-10}$  esu),  $m_e$  is the electron mass ( $9.1 \times 10^{-28}$  gm) and  $c$  is the free space velocity ( $3 \times 10^{10}$  cm/s).

The term,  $\omega_N$ , is the angular plasma frequency of the ionosphere and is given by

$$\omega_N^2 = \frac{4\pi N_e e^2}{m_e} \quad (\text{C-6})$$

where  $N_e$  is the electron density in electrons/cm<sup>3</sup>.

It should be noted that there are two values for the refractive index, Equation (C-1). The positive sign is associated with the ordinary wave while the negative sign with the extraordinary wave.

The quasi-longitudinal mode of propagation can be represented by the condition

$$4Y_L^2 (1 - X)^2 \gg Y_T^4 \quad (C-7)$$

It can be readily shown that, in order to maintain about a factor of 50 between the two terms, the approximation is valid when the propagation angle is restrained between  $0^\circ \leq \theta \leq 86.6^\circ$  at 100 MHz and  $0^\circ \leq \theta \leq 89.6^\circ$  at 400 MHz.

For the quasi-longitudinal case, the refractive index simplifies to

$$n^2 = 1 - \frac{X}{1 \pm Y_L} \quad (C-8)$$

Substituting Equations (C-2) and (C-4) in Equation (C-8), it follows that

$$n^2 = 1 - \frac{\omega_N^2}{\omega^2 \pm \omega_H^2 \cos \theta} \quad (C-9)$$

The condition for quasi-transverse propagation is denoted by the inequality

$$Y_T^4 \gg 4Y_L^2 (1 - X)^2 \quad (C-10)$$

which is merely the reverse of Equation (C-7). For this case, Equation (C-1) reduces to

$$n_o^2 = 1 - X \quad (C-11)$$

$$n_e^2 = 1 - \frac{X(1 - X)}{1 - X - Y_T^2} \quad (C-12)$$

where the subscripts, o and e, signify the ordinary and extraordinary waves, respectively.

Referring to Equation (C-8), the refractive index for the quasi-longitudinal mode of propagation can be written as

$$n^2 = 1 - X(1 \pm Y_L)^{-1} \quad (C-13)$$

Expanding by the binomial theorem, there results

$$n^2 = 1 - X \left[ 1 \mp Y_L + Y_L^2 \mp Y_L^3 + Y_L^4 \dots \right] \quad (C-14)$$

Further expansion can be accomplished by letting

$$n^2 = 1 - Z \quad (C-15)$$

Thus

$$n = 1 - \frac{1}{2} Z - \frac{1}{8} Z^2 - \frac{1}{16} Z^3 - \frac{5}{128} Z^4 \dots \quad (C-16)$$

where

$$Z = X \left[ 1 \mp Y_L + Y_L^2 \mp Y_L^3 + \dots \right] \quad (C-17)$$

$$Z^2 = X^2 \left[ 1 \mp 2Y_L + 3Y_L^2 \mp 4Y_L^3 + \dots \right] \quad (C-18)$$

$$Z^3 = X^3 \left[ 1 \mp 3Y_L + 6Y_L^2 \mp 10Y_L^3 + \dots \right] \quad (C-19)$$

In order words, the index of the refraction becomes

$$\begin{aligned} n = & 1 - \frac{1}{2} X \pm \frac{1}{2} X Y_L - \frac{1}{2} X Y_L^2 \pm \frac{1}{2} X Y_L^3 - \frac{1}{8} X^2 \\ & \pm \frac{1}{4} X^2 Y_L - \frac{3}{8} X^2 Y_L^2 \pm \frac{1}{2} X^2 Y_L^3 - \frac{1}{16} X^3 \\ & \pm \frac{3}{16} X^3 Y_L - \frac{3}{8} X^3 Y_L^2 \pm \frac{5}{8} X^3 Y_L^3 + \dots \end{aligned} \quad (C-20)$$

This expression can also be written in terms of the physical constants for X and Y<sub>L</sub>. Equations (C-2) and (C-4). It follows that

$$\begin{aligned}
 n = 1 - \frac{1}{2} \left( \frac{\omega N}{\omega} \right)^2 \pm \frac{1}{2} \frac{\omega^2 N^2 \omega_H}{\omega^3} \cos \theta - \frac{1}{2} \frac{\omega^2 N^2 \omega_H^2}{\omega^4} \cos^2 \theta \\
 - \frac{1}{8} \left( \frac{\omega N}{\omega} \right)^4 \pm \frac{1}{2} \frac{\omega^2 N^2 \omega_H^3}{\omega^5} \cos^3 \theta \pm \frac{1}{4} \frac{\omega^4 N^4 \omega_H}{\omega^5} \cos \theta + \dots
 \end{aligned} \tag{C-21}$$

The difference between the refractive indices of the ordinary and extraordinary waves is therefore

$$\Delta n = n_o - n_e = \frac{\omega^2 N^2 \omega_H}{\omega^3} \cos \theta + \frac{\omega^2 N^2 \omega_H^3}{\omega^5} \cos^3 \theta + \frac{1}{2} \frac{\omega^4 N^4 \omega_H}{\omega^5} \cos \theta + \dots \tag{C-22}$$